

Modeling the impact of drainage on peatland CO₂ and CH₄ fluxes and its underlying drivers

Liyang Liu¹, Philippe Ciais¹, Thu Hang Nguyen¹, Yi Xi¹, Chunjing Qiu², Elodie Salmon¹, Aram Kalthori³, Christophe Guimbaud⁴, Matthias Peichl⁵, Joshua L. Ratcliffe^{5,6}, Koffi Dodji Noumonvi⁵,
5 Xuefei Li⁷

¹Laboratoire des Sciences du Climat et de l'Environnement, IPSL, CEA-CNRS-UVSQ, Université Paris-Saclay, 91191 Gif sur Yvette, France

²Research Center for Global Change and Ecological Forecasting, School of Ecological and Environmental Sciences, East China Normal University, Shanghai, China

10 ³GFZ Helmholtz Centre for Geosciences, 14473, Potsdam, Germany

⁴Laboratoire de Physique et de Chimie de l'Environnement et de l'Espace, LPC2E, CNRS, OSUC, Univ Orleans, F-45071 Orléans, France.

⁵Department of Forest Ecology and Management, Swedish University of Agricultural Sciences, 90183 Umeå, Sweden

15 ⁶Unit for Field-Based Forest Research, Swedish University of Agricultural Sciences, 92291 Vindeln, Sweden

⁷Institute for Atmospheric and Earth System Research/Physics, Faculty of Science, University of Helsinki, 00014 Helsinki, Finland

Correspondence to: Liyang Liu (liyang.liu@lsce.ipsl.fr)

20 **Abstract.** Peatland drying is an important process affecting greenhouse gas (GHG) emissions. Ditching of peat for drainage to plant forest has been a widespread management practice in the Nordic countries, and drying increasingly occurs also from climate change induced drought. Previously published meta-analyses from literature suggest that drainage increases soil CO₂ emissions by enhancing oxic decomposition in aerated upper layers while suppressing CH₄ emissions. However, these data do not elucidate short-term variations of GHG fluxes during
25 drainage and usually only regress GHG emissions as a function of the annual mean water table. Here we developed a new parameterization of peat drainage in a land surface model that represents peat processes and fluxes of CO₂ and CH₄, by adding a machine-learning module to predict the daily water table depths from simulated soil moisture in the upper soil layers and a ditch that receives
30 drainage water. Because peatland pre-drainage GHG emissions vary between sites and influence subsequent changes following drainage, idealized simulations were performed for virtual drainage

applied to a collection of 10 pristine sites, where the model parameters are calibrated against observed GHG fluxes. Different drainage intensities are simulated by prescribing lower water table depths from setting the ditch depth from 5 to 80 cm below the initial water surface. The resulting
35 GHG flux changes across sites are compared with meta-analysis data from northern sites and show realistic results with a reduced CO₂ sink and reduced CH₄ emissions. Additional comparison with continuous flux data collected in the UK for different sites associated with increasing drainage levels also shows good model performance. Overall, using GWP100 to compare the effect of CH₄ vs. CO₂ flux changes, our model simulations suggest only small net GHG emission changes in CO₂-
40 equivalent GHG emissions under drainage scenarios over multi-decadal timescales, yet with differences between sites. Over time, simulated emission factors of CO₂ flux decrease because of exhaustion of labile soil organic substrate for decomposition, while reductions in CH₄ emissions are amplified due to decreased availability of material for anoxic decomposition. The sensitivities of CO₂ flux changes to increased water table depth changes are primarily controlled by initial CO₂ and
45 CH₄ fluxes, initial soil carbon content, peat vegetation community, air temperature and initial water table depth. The influence of peat vegetation on the GHG flux sensitivities in the model occurs via differing lability of soil organic carbon pools, with moss-dominated sites having a lower sensitivity due to their longer peat turnover time. Nonetheless, our calibrated global model remains limited in its ability to mechanistically represent drained peatland systems, particularly regarding
50 extrapolation and representation of dynamic soil and hydrological processes. Our model-simulated sensitivities of GHG fluxes to drainage can be approximated by linear regressions using site-level variables, which, despite the limitations, may offer a simplified, exploratory tool for estimating drainage effects.

1 Introduction

55 In peatlands, organic matter does not fully decompose due primarily to the lack of oxygen in the soil caused by waterlogged conditions. Peatlands have therefore accumulated a large amount of carbon over time, ~450Gt (Joosten, 2009; Page et al., 2011), though they also emit a significant amount of methane (CH₄) from anaerobic decomposition - commonly 5–80 mg m⁻² day⁻¹ in northern peatlands according to Blodau (2002). However, since the last few centuries, drainage of peatlands

60 has become widespread for various purposes, such as commercial forestry (Arnold et al., 2005),
farming (Kiew et al., 2020; Qiu et al., 2021), livestock grazing (Conchedda and Tubiello, 2020;
Nieveen et al., 2005), and peat extraction for fuel (Schilstra and Gerding, 2004; Sirin et al., 2010).
When peatlands are drained, increased oxygen levels in the soil promote aerobic decomposition of
organic matter, leading to higher CO₂ emissions into the atmosphere and reduced CH₄ emissions
65 (Holden, 2005; Rydin and Jeglum, 2013; Evans et al., 2021).

Field studies have been conducted to assess the impact of recent drainage on peatlands' contemporary greenhouse gas (GHG) emissions. Monitoring of recently drained sites using chambers (e.g., Furukawa et al., 2005; Laine et al., 2009; Martikainen et al., 1995; Munir et al., 2015; Strack and Waddington, 2007; Swails et al., 2022) and eddy covariance flux towers
70 (Tikkasalo et al., 2024; Tong et al., 2024) have been performed to measure GHG fluxes, but the amount of data is still scarce, limited to few sites and short-term duration (mostly < 10 years). When a site is being monitored which has been drained for a century, contemporary monitoring data observe the effect of drainage in the present, but as a consequence of biophysical and biochemical changes in the past. Apart from such contemporary diachronic observations of GHG fluxes at sites
75 that have been drained in the past, only few studies based on peat coring have actually been able to assess the impact of historic drainage.

In addition, meta-analyses gathering data from various sites and methods (Couwenberg et al., 2010; Maljanen et al., 2010; Prananto et al., 2020) have been combined with empirical upscaling models of drainage-induced GHG fluxes (Evans et al., 2021; Huang et al., 2021b) across diverse
80 geographic regions, peatland types and conditions. Meta-analyses consistently suggest that post-drainage peat decomposition causes long-term legacy CO₂ emissions, persisting decades after drainage (Couwenberg et al., 2010; Huang et al., 2021b; Zou et al., 2022). Concurrently, meta-analyses show that CH₄ emissions are reduced and N₂O emissions can be increased during drainage (Zou et al., 2022; Tikkasalo et al., 2024), the latter of which applies to N-rich sites.

85 Previous studies also showed that the mean water table level (WTL) under drained conditions controls the response of emissions, but there may be distinct WTL thresholds for each gas and for each peatland. For instance, Zou et al. (2022) found in their meta-analysis that CO₂ and N₂O

emissions only increase significantly when WTL is lowered by more than 30 cm below the soil surface. On the other hand, CH₄ emissions are suppressed when WTL is lowered to 5 cm below the soil surface, and then remain low for deeper WTL. Overall, using 100-year Global Warming Potential (GWP100) across multiple sites to compare CH₄ and N₂O with CO₂, Zou et al. (2022) showed that net CO₂-equivalent emissions are reduced by drainage when the WTL depth drops from being above the surface in inundated peat to 5 cm below the soil surface because of the predominant role of CH₄ reductions. When the WTL depth is below this typical threshold, net CO₂-equivalent emissions can increase with drainage from the increase of CO₂ emissions, offsetting the reduction of CH₄ emissions. However, those meta-analysis studies do not separate well site-specific responses, do not describe systematic effects of different initial conditions and initial water table depth during drainage. Due to the dominance of short-term drained experiments, data from meta-analysis do not offer a complete assessment of net climate effects caused by distinct decadal changes of CO₂, CH₄ and N₂O fluxes.

Another approach involves the use of process-based models, which can simulate the processes co-controlling CH₄ and CO₂ emissions by coupling water, thermal, and greenhouse gas biochemistry processes and drainage (Huang et al., 2021a; Kwon et al., 2022). Models are versatile, capable of simulating at various time scales and can be tailored to specific site conditions, though their reliance on generic parameterizations means they cannot always be precisely calibrated for individual sites (Liu et al., 2025). Yet, process-based models tend to be complex, and interpreting their results can therefore be challenging. Although process-based models have been increasingly applied to studying ecosystem GHG fluxes over the past decade, the majority of existing models are not specifically designed for peatlands (Mozafari et al., 2023), and their use in simulating peatland drainage was impossible. New peat-enabled land surface models have been applied at sites and over large regions using gridded simulations (Qiu et al., 2021) to study GHG fluxes of northern peatlands in response to climate changes and rising atmospheric CO₂, but the impact of drainage on GHG emissions has not been fully incorporated in these models. For instance, Qiu et al. (2021) used the ORCHIDEE-PEAT model to simulate peatland CO₂ flux changes for the historical conversion of northern peatlands to croplands and found a large cumulative loss of 70 PgC, but they prescribed to their model direct changes from peatland to cropland instead of considering a realistic transient

drainage period when the WTL is lowered and the peatland becomes altered for instance with soil compaction, followed by crop or pasture cultivation. Further, they did not study the effect of CH₄ emissions reduction after conversion to agriculture. Kwon et al., (2022) used a version of the same model that include CH₄ processes (Salmon et al., 2022) for simulating the effect of drier conditions at six Arctic peatland sites and found that lowering the water level by 10 cm reduced the CO₂ sink by $13 \pm 15 \text{ g C m}^{-2} \text{ year}^{-1}$ and decreased CH₄ emissions by $4 \pm 4 \text{ g CH}_4 \text{ m}^{-2} \text{ year}^{-1}$ leading to reduced accumulation of carbon over the next hundred years. For temperate peat sites, Evans et al. (2021) further showed from data that long-term water table drawdowns at most sites led to net carbon loss.

To our knowledge, there has not been any systematic modeling of the effect on GHG emissions of anthropogenic drainage of peatlands using land surface models that can simulate both CO₂ and CH₄ fluxes. One difficulty is that climate and pre-drainage fluxes and water levels are generally not measured continuously at sites subject to drainage, which prevents the calibration of models before the perturbation. In this study, we use the ORCHIDEE-PEAT, a land surface model developed to include peat processes for CO₂ and CH₄ fluxes to address this research gap. Our strategy is to provide idealized simulations to model virtual drainage conditions at 10 peatland sites in temperate and boreal regions (one in the US, one in Canada, one in Japan, and others in Europe) which are presently not subjected to intentional drainage using ditches. All the sites have continuous CO₂ observations from eddy covariance and 8 sites also have CH₄ flux observations from flux chambers. All the sites have continuous local hourly climate data used as model input and local water table depth measurements are also available at most sites. This set of well-observed sites allows us to calibrate the model before drainage. The changes of CO₂ and CH₄ emissions for different drainage intensities will be simulated by prescribing increasingly deeper water table depths. These drainage simulations will then be evaluated against meta-analysis results from northern temperate and boreal peatland sites (Huang et al., 2021b; Zou et al., 2022) and against a detailed set of flux measurements conducted across the UK by Evans et al. (2021) for different water table depths.

We performed idealized site simulations with virtual drainage in the future under current climate conditions, with different prescribed water table depths, as an exploratory modeling effort to investigate how peatland drainage processes can be represented within a land surface model and to identify key mechanisms, sensitivities, and structural challenges associated with drainage, rather

than aiming to provide fully validated predictive estimates of drainage impacts. Based on these simulations, we address the following questions: (1) what are the changes of CO₂ and CH₄ fluxes in response to drainage if we would drain even more peatlands and how do they compare with observations, (2) how do fluxes change as a function of drainage duration, (3) what is the modeled sensitivity of flux changes to water table depth, (4) what factors affect the sensitivity at each site in the model, (5) what is the net climate effect of CO₂ and CH₄ flux changes induced by drainage using the GWP100 metrics to compare CH₄ and with CO₂. There are other metrics such as GWP* (Lynch et al., 2020) and SGWP (Neubauer and Megonigal, 2015), but we use here the GWP100 as it is used by the UNFCCC and national inventories for comparing the two gases. In the following, we present the model and its modifications for simulating drainage (**Section 2**), the model performances for simulating baseline CO₂ and CH₄ fluxes and water table depth before drainage, and the results of idealized changes in fluxes during the drainage phase (**Section 3**). First, we compare the modeled flux changes to meta-analysis results and field measurements to evaluate the model results, ensuring that they fall within plausible ranges. Then, we simulate emission factors defined by the increase of CO₂ emissions and the decrease of CH₄ emissions over time for various durations of drainage. Finally, we analyze the sensitivities of CO₂ and CH₄ flux changes per unit of water table lowering in comparison with independent observations and analyze the factors that explain why the model has different sensitivities between sites. A discussion of our results, the model limitations for soil carbon dynamics and hydrological processes, and perspectives for future large-scale simulations are given in **Section 4**.

2. Methods

2.1 Peatland enabled land surface model

ORCHIDEE-PEAT is a land surface model (<https://orchidee.ipsl.fr/>) with a module specifically developed for peatland. In general, the model comprises two main components: (1) Energy and water balance, and (2) Vegetation and soil carbon cycle. In each model grid cell defining the spatial unit of simulation, the water balance is simulated individually for each soil tile containing a different type of vegetation, while the energy balance is simulated for the whole grid cell (Xi et

al., 2024). The soil hydrology is simulated using 11 vertical layers, considering incoming rainfall or snowfall, soil water evaporation, water infiltration in the soil profile every half-hour, surface runoff and drainage (also called subsurface runoff in similar models). One soil tile is specifically designated for peat with distinct soil hydrological parameters. To ensure that this peat soil tile keeps a high water content, bottom drainage is excluded and surface runoff from non-peat soil tiles is given to the peat soil tile at each time step, with a slab water layer that can be created above the peat soil surface of maximum thickness 10 cm. The vegetation and soil carbon cycle component calculates biogeochemical and biophysical variables for each plant function type (called PFT). A peatland tile can contain one or more specific PFTs that grow on it, with the possibility to prescribe a fraction of mosses, graminoids (= grasses + sedges) and shrubs.

The peatland percentage at a site is defined by the total fraction of peatland PFTs in the grid cell where the site is located. A more detailed description about the model can be found in Qiu et al. (2018) and Qiu et al. (2019). In addition, an improved routine for methane simulation for peatland was integrated into the model based on Salmon et al. (2022). This enables this study to analyze CO₂ fluxes and CH₄ emissions. The CO₂ flux represented by Net Ecosystem Exchange (NEE) is calculated as the algebraic sum of gross primary productivity (GPP, negative sign), autotrophic respiration (AR, positive sign), and heterotrophic respiration (HR, positive sign). A simplification is that lateral export of Dissolved Organic Carbon (DOC) and erosion removal of Particulate Organic Carbon (POC) are not represented. Methane produced in the soil layers is transported to the soil surface via plant-mediated transport, ebullition, and diffusion (positive sign), and methanotrophy is simulated in each soil layer from the modeled O₂ concentration.

Meteorological forcings used as input for the model (including precipitation, air temperature, air humidity, pressure, solar radiation, and windspeed) are extracted from the collection of CRUJRA forcing datasets (Friedlingstein et al., 2022). The 6-hour time resolution of CRUJRA data is automatically interpolated to 30 minutes (default time step) by the ORCHIDEE model.

2.2 Site description and simulation protocol

The idealized future drainage simulations will be implemented for 10 currently undisturbed peatland sites in temperate and boreal regions briefly described in **Table A1 (Appendix A)**. The

vegetation composition (graminoids, shrubs, and mosses) is taken from the literature when available; otherwise, it is estimated visually from satellite images.

The ORCHIDEE-PEAT model was first run for 100 years to reach the equilibrium state of soil thermal and hydrological conditions, followed by 10,000 years of spin-up to accumulate soil carbon with a fast module that computes only soil carbon changes from daily litter input and soil climate archived from the first simulation (Qiu et al., 2018), using repeated forcing data and a pre-industrial atmospheric CO₂ concentration of 285 ppm. An additional 100-year simulation was then conducted before flux observations (**Table A1**) to simulate biogeochemical processes under observed atmospheric CO₂ concentrations. The model was then calibrated for each site under present-day conditions following Liu et al. (2025), here calibrating the parameters controlling CH₄ fluxes in addition to CO₂ fluxes for sites that have CH₄ flux observation. For CO₂ fluxes, parameters governing photosynthesis rates, stomatal conductance, autotrophic respiration, soil organic carbon oxic decomposition rate and its sensitivity to temperature (**Table B1 in Appendix B**) were calibrated. For CH₄, we calibrated parameters driving the methane production, oxidation, and transport (**Table B1**). The calibration was performed using the ORCHIDEE data assimilation system (ORCHIDAS, Peylin et al., 2016), a Bayesian statistical framework, employing a genetic algorithm to minimize a cost function between observation and simulated outcomes (Tarantola, 2005), i.e. here between observed and simulated daily NEE, and daily CH₄ emission simultaneously. For sites without CH₄ flux observations, only CO₂ parameters can be calibrated, while parameters related to CH₄ processes were assigned using the average calibrated values from all sites with available CH₄ flux observations. After the calibration, to quantify the uncertainty from parameter values under current conditions affecting future predictions, we performed 10 Monte Carlo simulations by varying the temperature dependence of heterotrophic respiration (Q_{10}) and the oxygen deficit enhancement of methanogenesis (O_{2m}), which were found to be most influential controlling CH₄ emissions (Liu et al., 2025; Morel et al., 2019). Parameter uncertainty was then quantified as ± 1 standard deviation across these 10 simulations.

Pre-drainage simulations were run for each site over a period of 100 years. We then simulate five virtual idealized drainage scenarios for each site over a subsequent 50-year future period in which the water table remains at its initial level to define a baseline and varies each day from

230 hydrological balance simulations (no drainage), or is prescribed at 5, 10, 20, and 50 cm below the
initial/baseline water level. For the 150 years of simulations, 6-hourly climate forcings of the flux-
observed years are used by randomly selecting years. The same years are used for the undisturbed
and drained simulations to ensure that the resulting differences in fluxes are not caused by
differences in climate.

235 **2.2 Reconstruction of baseline water table**

Performing drainage simulations requires a good representation of the baseline water table
(WTD) before drainage. This is not straightforward in a model like ORCHIDEE where the
numerical discretization of the soil into layers is coarser with increasing depth, e.g. a layer has
thickness of 25 cm at 50 cm below the surface, which does not allow to position the water table in
240 this layer accurately, i.e. the model can capture broad seasonal WTD trends, but often struggles to
reproduce short-term fluctuation. Therefore, we developed a machine learning module, separate
from the ORCHIDEE model, to simulate the accurate position of the water table as a function of
simulated soil moisture in the soil layers, which leverages the WTD observation data that we have
for 8 out of 10 sites. It is expected to reconstruct a continuous and more detailed WTD time series
245 that aligns better with measured data, including finer temporal dynamics.

The module is trained to gap-fill the daily baseline water table observed at 8 sites and it is used
to reproduce the missing water table measurements at 2 sites (CZ-Wet, DE-Akm; **Table A1**).
Because the water table is closely related to soil moisture, our strategy is to extract the simulated
soil moisture of all the layers to train a model defined by $WTD = f(SM)$. Simulated soil moisture
250 and observed water table time series are sampled by 7-day blocks to make up the training dataset
for the model, with soil moistures as inputs and water table as output. Firstly, for a site where
observed water table data is available but with missing values, its own training dataset is divided
into an 80/20 ratio for training and testing, then the missing data are filled. This process is referred
to as self-reconstruction. Secondly, a multi-site training dataset is created using all the sites that
255 have water table observation with a training/testing ratio of 50/50 for four sites in Sweden and 80/20
for the remaining. The contribution of each Swedish site to the total training subset is reduced due
to their proximity to each other, which potentially results in the over-representation of their

relationships between water table and soil moisture when training the machine learning model. Once this multi-site model has been trained, it will take the simulated soil moisture (from ORCHIDEE-PEAT) of water-table-unknown sites as input to derive the baseline water table for these sites as output. In this study, we used a Support Vector Regression (SVR) model (Smola and Schölkopf, 2004) to learn and reconstruct the relationship between soil moisture and water table, because of its advantages such as robustness to outliers and effectiveness in high-dimensional space (Mohammed Rashid et al., 2022).

2.3 Peatland drainage by ditching

In order to simulate the effect of drainage on CO₂ and CH₄ fluxes, we assume that the water table is lowered by draining into ditches. We introduce into the model a new module with a ditch of which depth is the same as the desired lowered maximum water table depth (e.g., if the lowest water table under drainage is 40cm, then ditch depth is 40cm). In addition, runoff from other soil tiles to peat is assumed to be excluded during drainage implementation, reducing water supply to peat. Note that the simulated water table fluctuates continuously throughout the year from variable incoming rainfall, and so does the ditch water level. The difference in the hydrology simulations with and without drainage is shown in **Figure 1** and described below.

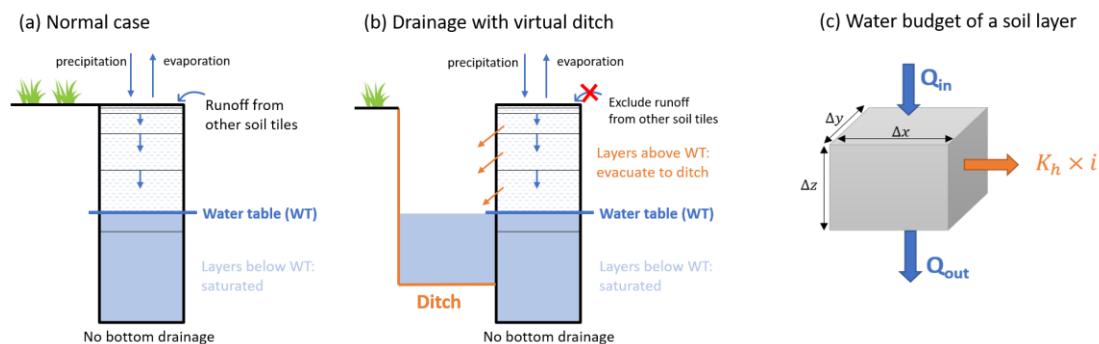


Figure 1. Illustration of drainage by ditch simulation in the ORCHIDEE-PEAT model: (a) Soil column without a ditch, showing vertical water fluxes and horizontal delivery from the runoff of adjacent soil tiles without peat. (b) Soil column with a ditch, incorporating lateral water loss to the ditch (orange) and suppression of runoff from other tiles. (c) Water budget of a soil layer, with lateral output fluxes due to drainage into the ditch highlighted in orange. The dimension of the volume of soil is defined by Δx , Δy and Δz . Q_{in} and Q_{out} are inward and outward water fluxes and K_h is the horizontal hydraulic conductivity and i is the hydraulic gradient.

In the ORCHIDEE model, each soil column is separated into layers. We set soil layers below the water table to be saturated ($\theta=\theta_s$). Above the water table, in a volume of soil with horizontal dimension $\Delta x, \Delta y$ and thickness Δz , without drainage, water flows through the soil in the vertical dimension from the infiltration of rainfall events and runoff given by other soil tiles in the same grid (Fig. 1a, blue arrows), a flux Q_{in} entering and a flux Q_{out} leaving the layer across the cross-section area $\Delta x \Delta y$ (Fig. 1c). These vertical fluxes are functions of hydraulic conductivity and diffusivity (K_v [$m\ s^{-1}$] and D_v [$m^2\ s^{-1}$], respectively, with v for vertical) which are functions of soil moisture ($\theta^{t+\Delta t}$).

With drainage, a new horizontal flux across the cross-section area $\Delta y \Delta z$ is added to represent water running out of the soil to the ditch (Fig. 1c, orange arrow). Assuming that ditches are placed perpendicularly to the flow of groundwater, this additional drainage flux is a function of horizontal hydraulic conductivity (K_h) and hydraulic gradient (i). The change of moisture in a time step Δt is given by:

$$\frac{\Delta \theta}{\Delta t} \Delta x \Delta y \Delta z = (Q_{in} - Q_{out}) \Delta x \Delta y - (K_h i) \Delta y \Delta z \quad (1)$$

Removing $\Delta x \Delta y$ in both sides, Eq. (1) becomes:

$$\frac{\Delta \theta}{\Delta t} \Delta z = (Q_{in} - Q_{out}) - (K_h i) \frac{\Delta z}{\Delta x} \quad (2)$$

with Δx now playing a role as ditch spacing. Using a numerical method with boundary conditions at top layer where Q_{in} = (precipitation - soil evaporation) and at bottom layer where Q_{out} = free drainage = zero, a tridiagonal matrix system is constructed to solve $\theta^{t+\Delta t}$ (Ducharne et al., 2018). Note that in the ORCHIDEE model, vertical water fluxes are simulated only in the downward direction – from the surface layer to lower soil layers. Upward water movement due to capillary forces is not currently represented in the model. Lateral subsurface water fluxes are also not represented.

305 **3 Results**

3.1 Simulation before drainage

The results of the model calibration under present conditions are shown in **Fig. 2**, with CO₂ fluxes (Net Ecosystem Exchange, NEE) and CH₄ emissions calibration for sites that have observations of both fluxes (a-h), and CO₂-only calibration for other sites (i-j). The CH₄ fluxes of all eight sites were well simulated, with RMSE ranging from 0.017 to 0.025 g CH₄ m⁻² day⁻¹. The calibrations of NEE also showed good performance, with RMSE smallest at Sweden sites (from 0.585 to 0.691 g CO₂ m⁻² day⁻¹).

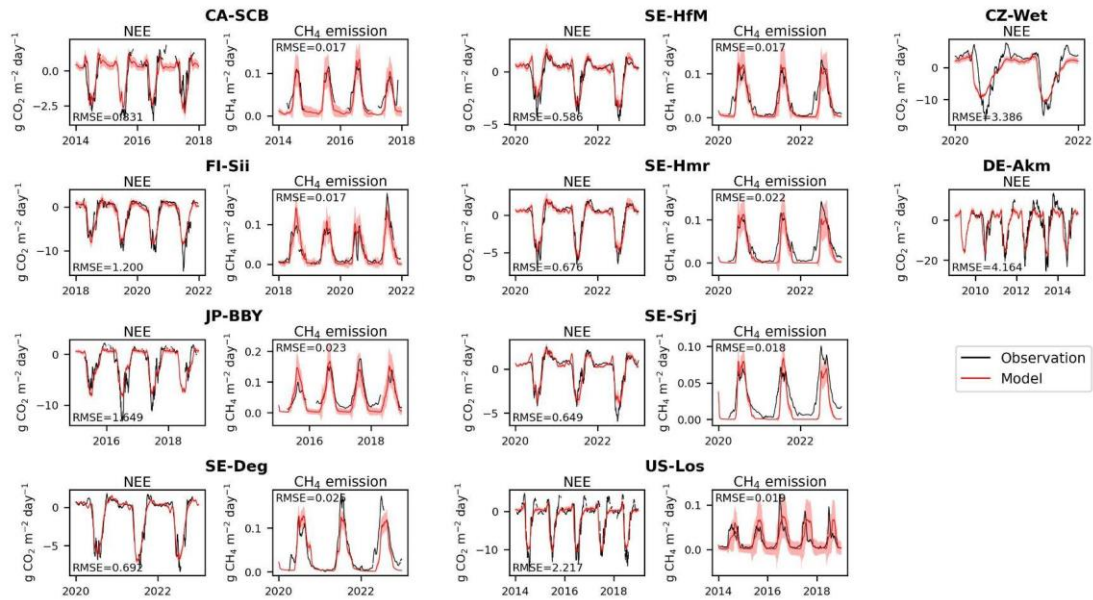


Figure 2. Comparison of model simulations after calibration with observed net ecosystem exchange CO₂ fluxes (NEE) and CH₄ emissions. Sites in panels a-h measured both fluxes and in i-j only NEE. The red shadings in each plot represent the uncertainty (± 1 standard deviation across 10 Monte Carlo simulations; see Methods) in the simulated NEE or CH₄ emission induced by parameter uncertainty.

Figure 3 presents the reconstruction of water table depth from soil moisture with the SVR model trained for individual sites (**Fig. 3 a-h**, left column). The RMSE of modelled and observed water table depth ranged from 2.76 cm (FI-Sii) to 6.11 cm (US-Los) and the model captured in general the seasonal variations very well, though less so the short-term variations. At the Swedish

325 sites, the peat is frozen between mid-October to early May, during which time the WTD is not
fluctuating in reality. However, due to the lack of WTD measurements during these frozen periods,
the self-reconstructed WTD from the SVR model for these times were accepted as the best available
approximation. With the SVR model trained using all the sites together, SVR was less effective
because it must compromise the patterns between all the sites: RMSE increased up to 6.76cm but
still captures the main seasonal variations. The water table depth reconstructed using SVR trained
330 from all other sites and applied at the two sites where direct WTD observations were missing
including CZ-Wet, DE-Akm (**Fig. 3 i-j**, right column) was used in this study as the baseline water
table depth.

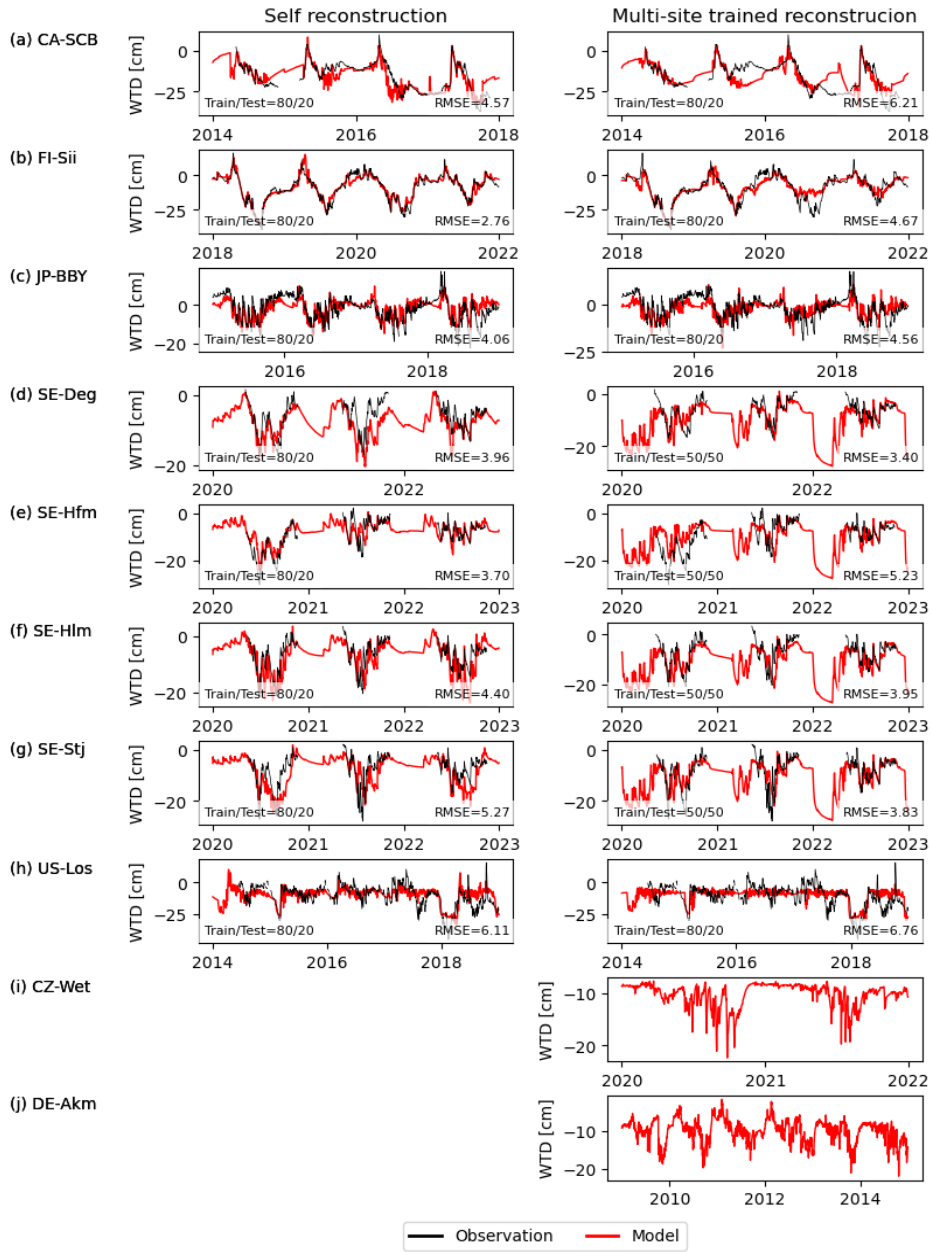
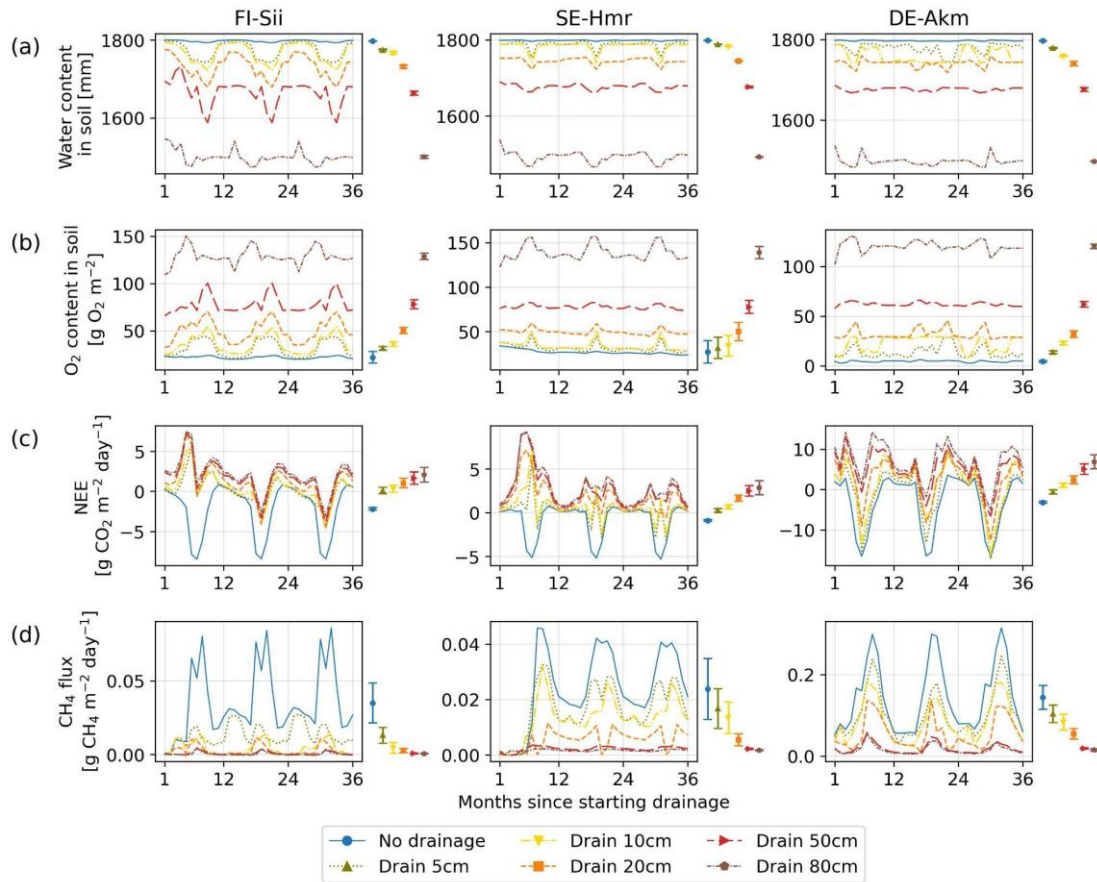


Figure 3. Water table depth reconstruction with a machine learning model trained on observations and using modelled soil moisture in all soil layers within the top 2 meters below the surface (red) compared with observed values (black).

335

3.2 Drainage simulation: changes of CO₂, CH₄ fluxes, soil water and oxygen after few years

Drainage reduced the water content in the soil and increased oxygen concentration (**Fig. 4**). With more oxygen in the soil and less moisture, heterotrophic respiration was increased. On the contrary, methane production was suppressed in aerated soil, leading to less methane emission when the water table gets deeper. **Figure 4** presents the monthly average of soil water content, oxygen, NEE and CH₄ emissions during the first three years after drainage, for different WTD levels. It shows that the inclusion of a ditch in the model could lower soil moisture effectively and that flux simulation responded as expected with decreased NEE uptake or NEE switching to a net CO₂ source, and decreased CH₄ emissions. Note that there could be a slight inconsistency between the pre- and during-drainage simulations. In the pre-drained simulation, soil moisture was calculated by the model, whereas in the drainage simulation, all the soil column below the ditch depth was forced to be saturated, which introduces a different water content of the deep layers. For instance, a deep layer that was near-saturated in the pre-drainage simulation was set to become saturated in the drainage simulation. The impact of this inconsistency on gas fluxes, however, was small because deep layers did not contribute much to changes in CH₄ and CO₂ fluxes (they contain less labile organic carbon) and they were already near-saturation or at full saturation before drainage. The 50-year time series of NEE and CH₄ emissions are shown in **Figure C1 (Appendix C)**.



355 **Figure 4.** Simulated changes at three sites of (a) soil water content in the whole profile (2m), (b)
 360 soil oxygen content, (c) Net Ecosystem Exchange of CO₂ and (d) methane emissions. Different
 colors indicate different water table depths below the original water level at each site. The coloured
 bars on the right of each panel summarize parameter uncertainty, quantified as ± 1 standard deviation
 of the simulated time-mean fluxes computed over the full 50-year drainage simulation from 10
 Monte Carlo runs. The coloured dots indicate the time - mean flux simulated using the calibrated
 parameter set. Note that when a flux (e.g. CH₄) is close to zero, the corresponding parameter-
 induced uncertainty also approaches zero.

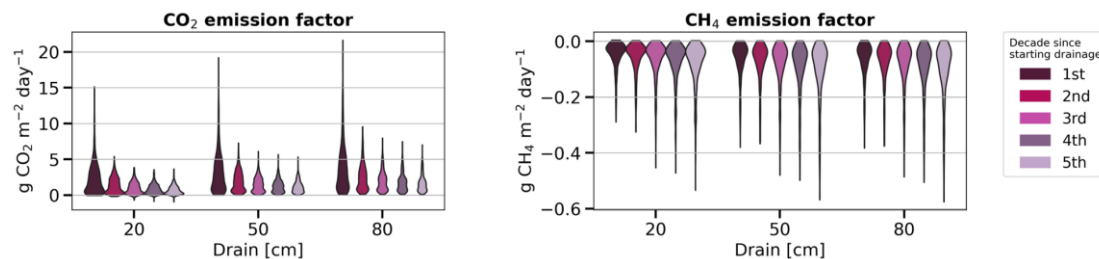
3.3 Long-term changes of CO₂ and CH₄ fluxes, diagnosed by emission factors after up to 50 years

365 **Figure 5** shows the average emission factor (EF) across all peatland sites for 50 years since
 starting the idealized drainage scenarios. The EF is defined by the average GHG flux per unit of

area over a given period of time under drainage minus the flux at the same site under undisturbed conditions. Qiu et al. (2021) implemented similar calculations using the ORCHIDEE-PEAT model for estimating carbon emission factors after peatland cultivation. Their emission factors calculated
370 over two decades following conversion of peatland to cropland was $16 \text{ g CO}_2 \text{ m}^{-2} \text{ day}^{-1}$ as a median, ranging from 5 to more than $50 \text{ g CO}_2 \text{ m}^{-2} \text{ day}^{-1}$. Our estimates are lower than their values, with a median of $2.56 \text{ g CO}_2 \text{ m}^{-2} \text{ day}^{-1}$ (95% CI: 0.35 to 10.71) for 80-cm drainage (**Fig. 5**). Our lower median EF values than Qiu et al. (2021) are because deep soil layers remain saturated in our simulations, preserving their carbon from decomposition, while Qiu et al. (2021) assumed that the
375 entire soil profile became drained and under-saturated when converting to cropland.

Regarding the temporal variation of emission factors, we found a decrease in CO_2 EF between the first and the fifth decade (**Fig. 5**) from $3.82 \text{ g CO}_2 \text{ m}^{-2} \text{ day}^{-1}$ (0.36 to 12.76) down to $1.65 \text{ g CO}_2 \text{ m}^{-2} \text{ day}^{-1}$ (0.29 to 4.57) for 80 cm drainage, a similar trend than the findings of Qiu et al. (2021). As GPP and autotrophic respiration (AR) was found to be little affected during the drainage period (**Fig. C2 f and g**), the change in emission factor over time was primarily driven by the increase of heterotrophic respiration (HR) under drainage compared to undrained conditions (**Fig. C2e**). HR includes one part from litter and one from soil. In the early decade, the decomposition of litter accelerated in the case of drainage, leading to the quick decrease in litter amount (**Fig. C2a**). Later, the reduced availability of litter for decomposition caused the heterotrophic respiration from litter
385 in drained peatlands to approach the same levels than in undrained peatlands (**Fig. C2b**) where litter accumulated gradually, or decomposed at a much slower rate, and maintained a stable and low heterotrophic respiration rate. On the other hand, while SOC in undrained peatlands accumulated gradually, SOC in drained peatlands increased rapidly in the early decades due to a large input of carbon from litter but then slowed down as litter carbon input declined (**Fig. C2c**). Consequently,
390 the difference in soil heterotrophic respiration (HR) between drained and undrained peatlands narrowed over time (**Fig. C2d**). These declining trends of both soil and litter HR in drained peatlands explain why the simulated EF decreased by time. A small decreasing trend in EF over time following drainage was determined experimentally by Truskavetskii (2014) based on soil measurements from chronosequence data. Rojstaczer and Deverel (1993) reported a trend in the subsidence of organic
395 soil over time using periodic leveling surveys, suggesting decreased EF as well, although our model

did not explicitly include subsidence and compaction effects. For CH₄ emissions, on the contrary, the decrease of EF amplifies with time, going from -0.07 g CH₄ m⁻² day⁻¹ in the first decade down to -0.10 g CH₄ m⁻² day⁻¹ in the last decade in the case of 80 cm drainage as shown in **Fig. 5** (negative EF in this Figure indicating less CH₄ emissions in the drained than in the undrained).



400

Figure 5. Evolution of modelled emission factors (a) for CO₂ fluxes and (b) for CH₄ emissions for five decades after drainage, displayed for three drainage depths. Negative values in the right plot indicate less CH₄ emissions in the drained condition than in the undrained condition.

3.4 Comparison of simulated greenhouse gas flux changes with observations

405

To evaluate our drainage simulation results for GHG fluxes, we used observed changes of CO₂ and CH₄ fluxes collected from multiple sources through two meta-analyses of drained wetlands experiments (Huang et al., 2021b; Zou et al., 2022), the network of field flux measurements collected in Europe by Evans et al. (2021), and measurement collected in the dataset of Ecosystem Services publicly provided by the WET HORIZONS project

410

(<https://www.wethorizons.eu/resources/#database>). Water table depths were provided along with the fluxes in both meta-analysis studies, while in Evans et al. (2021), an 'effective' water table depth was used, defined as the smaller value between the measured water table depth and the measured peat depth. The data collected by Huang et al., (2021b) provided measurements of undisturbed fluxes at control sites, as well as 77 measurements of fluxes after < 1 year, 42 after 1-10 years, and

415

78 after > 10 years of drainage. Since measurements taken within 10 years of drainage seem to dominate, we compared 10-years average values of our simulation with these data. **Figure 6a and b** shows the distribution of simulated and observed NEE and CH₄ fluxes for different water table levels, regardless of the site and drainage level, excluding CH₄ fluxes from CZ-Wet and DE-Akm, which were not calibrated during the pre-drainage period. Overall, our simulation results lie within

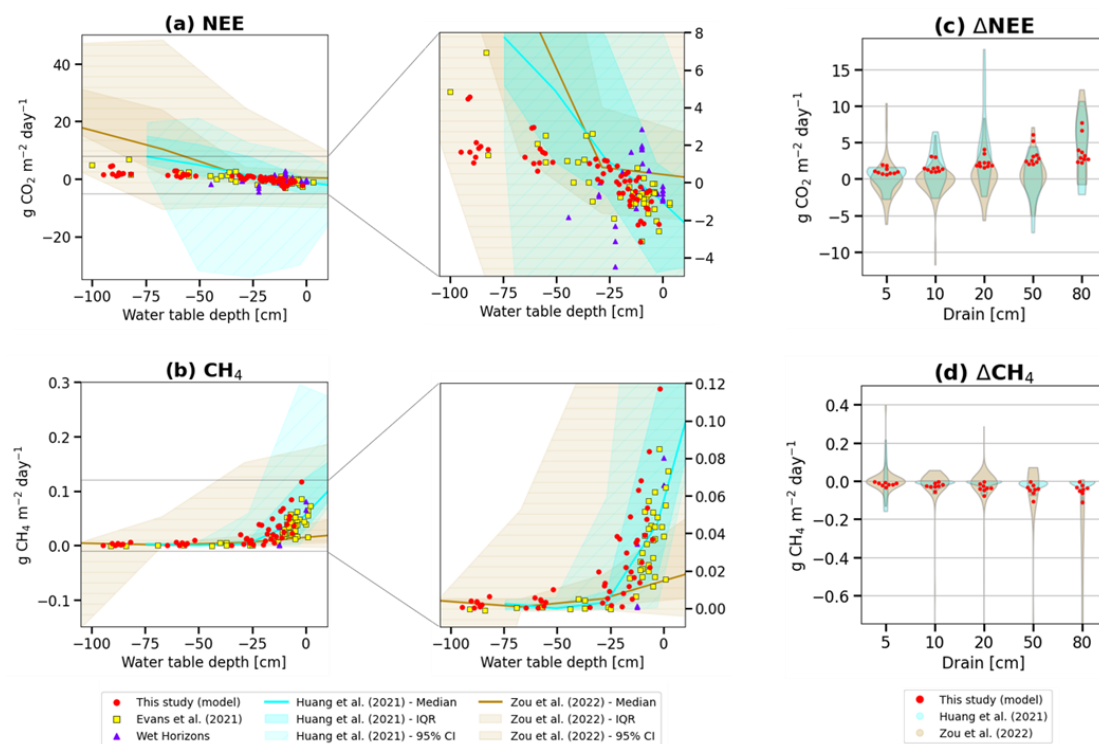
420

the large range of the observed data, although our modeled CH₄ emissions are in the upper range of

the observed distribution. In Evans et al. (2021), a linear relationship was obtained between effective water table depth and net ecosystem production (NEP, the sum of NEE and biomass removal). Retaining only sites within boreal and temperate zones from their study (the yellow points in **Fig 6a and b**), we found that our model, despite its simplified hydrology, can reproduce such a strong linear correlation between effective WTD and NEE ($NEE = -0.062 \times WTD - 1.425$, $R^2=0.66$, $p<0.001$). Our results (the red points in **Fig 6a and b**) were in good agreement with Evans et al. (2021), yet a smaller slope between WTD and NEE was obtained in the model ($NEE = -0.041 \times WTD - 1.060$, $R^2=0.64$, $p<0.001$). Meta-analysis data mixing different sites, experiment duration and conditions showed a weak correlation ($R^2 = 0.04$ in Huang et al. (2021b), and $R^2 = 0.18$ in Zou et al. (2022)), suggesting that the Evans et al. (2021) field measurements with continuous flux and WTD records at the same site may be a better benchmark of the model results.

The distributions of the changes of fluxes compared to no drainage are presented in **Figure 6c and d** for different drainage levels (ΔWTD). For this comparison, we kept only samples for 5, 10, 20, 50, and 80 cm ($\pm 10\%$) drainage levels in the reference data. The numbers of measurements for each drainage level differs and different drainage levels can include different peatland sites and types. The results indicate that the modeled distribution of ΔNEE falls within the observed distributions from Huang et al. (2021b) and Zou et al. (2022), although all of our simulations show positive ΔNEE values ranging from 0 to $7.70 \text{ g CO}_2 \text{ m}^{-2} \text{ day}^{-1}$, i.e., more CO_2 is emitted or less CO_2 absorbed after peatlands are drained, whereas the meta-analysis data exhibit either increases or decreases of NEE (-7.33 to $17.80 \text{ g CO}_2 \text{ m}^{-2} \text{ day}^{-1}$ in Huang et al. (2021b), and -11.75 to $12.26 \text{ g CO}_2 \text{ m}^{-2} \text{ day}^{-1}$ in Zou et al. (2022)). For methane, all ΔCH_4 values are negative in our model, ranging from -0.11 to $0 \text{ g CH}_4 \text{ m}^{-2} \text{ day}^{-1}$, i.e. less CH_4 is emitted when peat is drained, while the meta-analysis data shows a negative median value of the distribution, yet with negative or positive changes of ΔCH_4 (-0.16 to $0.22 \text{ g CH}_4 \text{ m}^{-2} \text{ day}^{-1}$ in Huang et al. (2021b); -1.27 to $0.40 \text{ g CH}_4 \text{ m}^{-2} \text{ day}^{-1}$ in Zou et al. (2022)). These discrepancies mainly come from the fact that the meta-analysis studies took into account emission variations for different WTDs which can come from natural climate, microtopographic conditions and laboratory experiments, while our study focuses on ditch drainage conditions. For example, Huang et al. (2021b) included a comparison between a lawn with near-surface WTD and an adjacent hollow filled with water, which gave a negative ΔNEE because

450 the hollows leached dissolved or particulate organic carbon, facilitating oxidation, thus releasing more CO₂ than the lawn (Villa et al., 2019). A decrease in NEE may also result from anomalously cold weather, which can reduce respiration more significantly at the drained site than at the undrained site (Renou-Wilson et al., 2016), given that dry soil is more susceptible to air temperature fluctuations, and low temperatures inhibit soil decomposition. Additionally, inconsistencies in the data may contribute to their large range of ΔNEE, as they include different drainage levels and varying durations. Potential errors in the meta-analysis studies, such as inconsistencies in data collection, may also play a role in estimating negative ΔNEE or positive ΔCH₄; for instance, our inspection of meta-analysis data found cases where emission data reported for different depths were from different locations.



460

Figure 6. Simulated fluxes of (a) Net ecosystem exchange of CO₂ and (b) CH₄ emissions for different water table levels below the original water surface (red points) compared with meta-analysis observations from Huang et al. (2021b) (cyan) and Zou et al. (2022) (brown), and with field measurements from Evans et al. (2021) (yellow) and WET HORIZONS project (purple). The darkest color shading represents ±1 standard deviation across observed sites, and the lightest

465

shading indicates the minimum–maximum range of the observations. (c) Modeled (red dots) and observed distributions of NEE changes (Δ NEE) for different water table depths of drainage, compared with meta-analysis results, and (d) same for CH₄ emissions changes (Δ CH₄). For consistency with observational datasets, model results were averaged over the first 10 years of simulations, corresponding to the period during which most post-drainage observations were collected.

3.5 Sensitivity of GHG emissions changes to lowered water table depth

In this section, we analyzed the *sensitivity* of GHG fluxes defined by the change of NEE or CH₄ emission per cm of lowered WTD computed from our simulations, for different starting WTD levels at the same site, after 10 years of drainage. For the observations, we calculated the sensitivities from changes in GHG emissions reported by Huang et al. (2021b) and Zou et al. (2022) and changes in WTD between 5 and 80 cm. The distributions of the resulting sensitivities are shown in **Fig. C3**. Averaged across all sites, the modeled mean NEE sensitivity ($0.07 \text{ g CO}_2 \text{ m}^{-2} \text{ day}^{-1} \text{ cm}^{-1}$; 95%CI: 0.01 to 0.28) is close to the observation-based values derived from the data of Huang et al. (2021b); $0.12 \text{ g CO}_2 \text{ m}^{-2} \text{ day}^{-1} \text{ cm}^{-1}$; -0.23 to 0.67), but higher than the data of Zou et al. (2022), although within their 95% confidence interval ($0.01 \text{ g CO}_2 \text{ m}^{-2} \text{ day}^{-1} \text{ cm}^{-1}$; -0.37 to 0.43). The simulated methane emission sensitivity ($-1.43 \text{ mg CH}_4 \text{ m}^{-2} \text{ day}^{-1} \text{ cm}^{-1}$; -6.73 to 0.0) is also comparable to the empirical values ($-1.82 \text{ mg CH}_4 \text{ m}^{-2} \text{ day}^{-1} \text{ cm}^{-1}$; -15.75 to 0.17 of Huang et al. (2021b) and $-1.71 \text{ mg CH}_4 \text{ m}^{-2} \text{ day}^{-1} \text{ cm}^{-1}$; -19.47 to 5.02 of Zou et al. (2022). Kwon et al. (2022) used ORCHIDEE for 100-years drainage simulations at six arctic peatland sites with WTD lowered by 5 to 50 cm and reported average sensitivities of $0.01 \pm 0.02 \text{ g CO}_2 \text{ m}^{-2} \text{ day}^{-1} \text{ cm}^{-1}$ for NEE, and of $-1.10 \pm 1.10 \text{ mg CH}_4 \text{ m}^{-2} \text{ day}^{-1} \text{ cm}^{-1}$ for CH₄ emissions. Our modeled NEE sensitivity is more positive and our modeled CH₄ emission sensitivity is slightly more negative than Kwon et al. (2022), despite using almost the same model. This may be attributed to the fact that we did simulation across a larger range of climate while Kwon et al. (2022) only simulated drainage of arctic wet peatlands where winter respiration is absent and high rainfall and snowmelt inputs maintain relatively more stable hydrological conditions, thus their NEE and CH₄ emissions are less sensitive to lowered WTD.

Instead of fitting a linear regression between all the flux changes and all the WTD changes in the simulations (for **Fig. 6c and d**), we calculated the sensitivity as the change of flux divided by

the change of WTD ($\frac{\Delta flux}{\Delta WTD}$) for each possible pair of flux and negative water tables changes, i.e. when WTD becomes deeper, like in Huang et al. (2021b). The ‘starting’ water table depth in the x-axis of **Fig. 7** is the shallower WTD in ΔWTD used to calculate sensitivities. This starting water table level can be taken from a drained simulation, and thus differs from the ‘initial’ water table which corresponds to undisturbed conditions. The results shown in **Fig. 7** indicate that the more shallow is the starting WTD, the higher are the sensitivities of NEE and CH₄ emissions fluxes when the WTD is further lowered. This is because when drainage is applied to a site with a shallow starting water table, it affects upper soil layers that were previously saturated and causes large emissions changes. Conversely, if drainage is applied to a site with a deep starting water table, upper layers that were already exposed to oxygen experience minimal change and deeper layers dry out but the SOC that they contain decomposes more slowly (they contain more slow and passive carbon with slower turnover time in the model), resulting in a smaller sensitivity of fluxes. The sensitivities of NEE is a non-linear function of starting WTD (non-linear AIC = -824 < linear AIC = -820, with AIC definition in **Appendix C**). CH₄ emissions sensitivity also depends on a non-linear manner of the starting WTD (non-linear AIC = -1935 < linear AIC = -1928 for CH₄ emission) and tends to saturate when drainage starts from a deep water table. The sensitivity of CH₄ emissions increases from negative values to almost zero when the starting WTD is deeper than ≈ 40 cm.

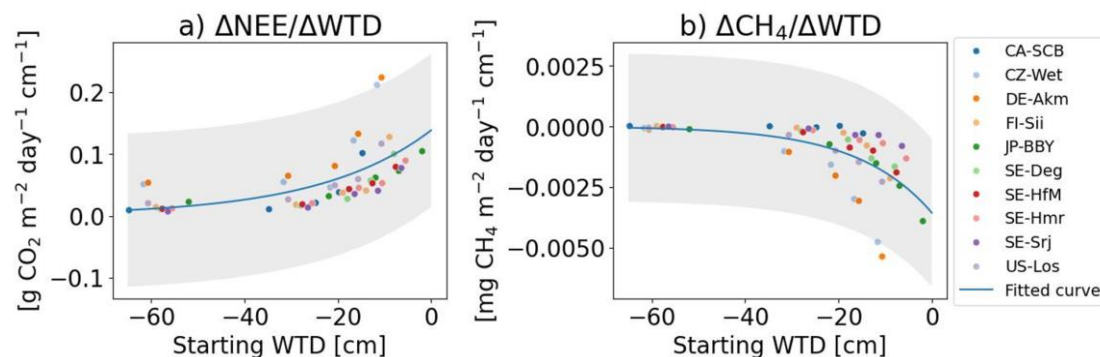


Figure 7. Sensitivities of (a) net ecosystem exchange ($\Delta NEE/\Delta WTD$) and (b) CH₄ emissions ($\Delta CH_4/\Delta WTD$) to water table depth as a function of the starting water table depth. The starting water table depth is the upper value in ΔWTD used to calculate sensitivities by dividing $\Delta flux$ by ΔWTD for all possible negative values of ΔWTD . The analysis is performed based on results from the first 10 years of drainage simulations. The grey shadings represent 95% CI of the regression.

3.6 Factors controlling the sensitivity of GHG emissions to water table depth across sites

520 **Figure 8** shows the simulated sensitivities ($\frac{\Delta flux}{\Delta WTD}$) of the 10 sites after 10-years of drainage, together with other model variables that could plausibly explain their values. For clarity, the sensitivities are shown in rank from the highest to the lowest for NEE (**Fig. 8a**). The regression between sensitivities and each of the selected model variables (**Fig. 8 c-h**) are shown in **Fig. 9**.

525 Firstly, we analyzed whether the sensitivities depend on the magnitude of the initial fluxes, based on the hypothesis that a site with a higher baseline flux before drainage would experience more drastic changes during drainage. Among all sites, DE-Akm and CZ-Wet had the highest sensitivities of NEE (0.14 and 0.12 g CO₂ m⁻² day⁻¹ cm⁻¹, respectively, **Fig. 8a**). These two sites, along with JP-BBY, also exhibited the greatest CH₄ emissions sensitivities (-3.17, -2.85, and -2.37 mg CH₄ m⁻² day⁻¹ cm⁻¹, **Fig. 8b**). These sites were all characterized by the largest initial CO₂ sinks and CH₄ emissions before drainage. Conversely, the site with the smallest pre-drainage CH₄ emissions, CA-SCB, had the smallest CH₄ sensitivities. SE-Srj has the smallest NEE sensitivities with the smallest initial NEE. Overall, we found that the CH₄ sensitivities show a very strong linear relationship with initial CH₄ emissions ($R^2 = 1$, $p < 0.001$) across sites. Similarly, the NEE sensitivities are correlated with the initial NEE, but the relationship is weaker ($R^2 = 0.71$, $p = 0.002$)
530
535 (**Fig. 9, top row**).

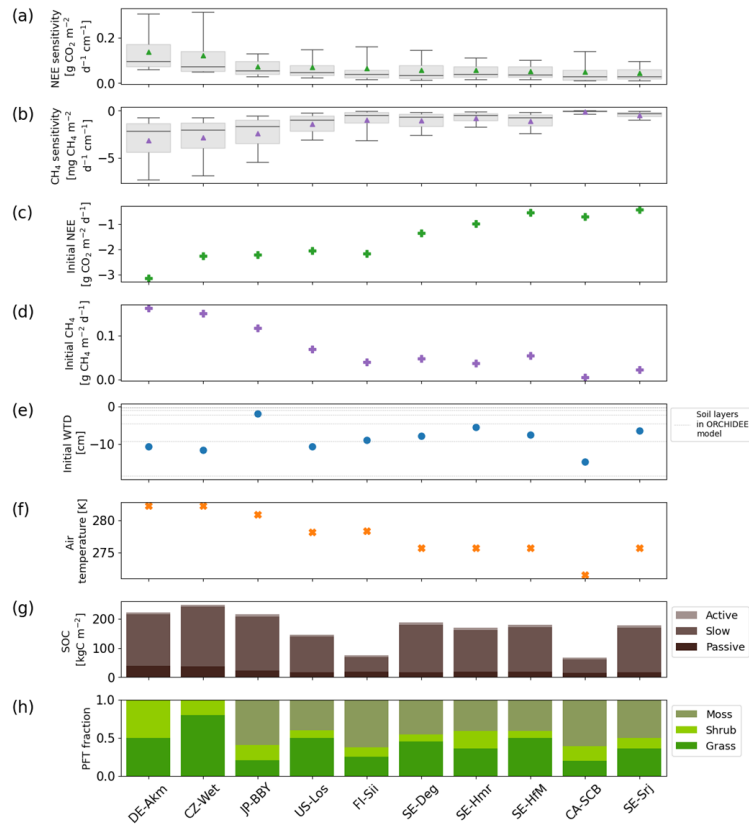


Figure 8. Summary of site-level sensitivities and explanatory variables used to analyze the drivers of drainage responses. (a) Sensitivity of NEE to water table drawdown at each site, expressed as the change in flux per centimeter of deeper water table depth ($\Delta\text{NEE}/\Delta\text{WTD}$); positive values indicate reduced CO_2 uptake or net emissions with deeper WTD, (b) same as (a), but for CH_4 emissions ($\Delta\text{CH}_4/\Delta\text{WTD}$); negative values indicate reduced CH_4 emissions with deeper WTD. (c) Initial NEE, (d) initial CH_4 emissions prior to drainage. Additional modeled variables examined for their role in explaining the sensitivities include (e) initial water table depth prior to drainage (negative values indicate water table below the surface), (f) annual mean air temperature, (g) modeled soil organic carbon density (SOC), calculated as the sum of active, slow, and passive pools over the full soil column, and (h) peatland vegetation composition including peatland graminoids, shrubs, mosses. All statistics are based on modeled results from the first 10 years of drainage simulations, consistent with the temporal window used for sensitivity analysis.

Secondly, we examined if the vegetation composition of each site affects the sensitivities when the site is drained. To quantify this response, we calculated a moss index (MI) defined by the ratio $\frac{\text{moss} - \text{grass} - \text{shrub}}{\text{moss} + \text{grass} + \text{shrub}}$ so that it is equal to -1 in absence of moss and to 1 with full moss cover, and

found a negative correlation between MI and NEE sensitivity ($R^2 = 0.75$, $p < 0.001$), and a positive correlation between MI and CH_4 emission sensitivity ($R^2 = 0.65$, $p = 0.01$) (**Fig. 9 a and b**, last items). We identified two mechanisms in the model that explain this response of sensitivities to the moss fraction. The first mechanism is that a higher moss fraction is associated with less decomposable organic carbon. Among the three types of peatland vegetation, soil organic carbon decomposes the slowest for mosses and the fastest for shrubs, with residence times of 2 years for moss, 1 year for grass/sedges, and 200 days only for shrubs at $>30^\circ\text{C}$, for the active soil organic carbon pool of the model. Accordingly, we found that the sites with higher fractions of shrubs and lower fractions of mosses display higher sensitivities of NEE to drainage (**Fig. 8**). The methane emission sensitivities depend on vegetation cover in a different way. Peatland sites with mosses have shallower effective root depths (1-5 cm), reducing plant-mediated methane transport in the model, and the opposite is true for grasses/sedges and shrubs (root depth $\approx 30 - 50\text{cm}$). Most of the sites in this study have an initial mean WTD already below 5 cm, i.e. deeper than the depth at which mosses typically facilitate methane transport. When the WTD gets deeper, plant-mediated transport of methane by moss is thus not strongly affected in our model. Sites with more mosses (e.g. CA-SCB) therefore show smaller methane emission sensitivities. The second mechanism is that the moss fraction regulates the initial amount of SOC, which partly explains the differences in sensitivities shown in **Fig. 8**. Note as well that moss-dominated sites have a higher potential for oxidation of CH_4 due to a symbiosis between mosses and methanotrophic bacteria (Larmola et al., 2010), but our methanotrophy module does not simulate this effect. Sites dominated by shrubs and grasses/sedges (DE-Akm, CZ-Wet) accumulate more SOC before drainage. When drainage exposes the upper peat soil layers to oxygen, accelerating soil respiration and limiting methane production, these sites with larger initial SOC pools show a larger increase in CO_2 emissions and a larger decrease of CH_4 emissions compared to moss-dominated sites (CA-SCB, FI-Sii).

Thirdly, we analyzed how the sensitivities depend on the initial WTD across all the sites. We found that the shallower the initial water table, the higher the sensitivities of NEE and CH_4 emissions. This result is qualitatively consistent with the data shown in **Fig. 7** where all sites are displayed together, but it additionally indicates that the site to site differences of sensitivities are partly explained by the variability of initial water table values ($R^2 = 0.36$, $p < 0.001$ for NEE; $R^2 = 0.54$,

$p=0.02$ for CH_4 emissions) (**Figure 9a and b, middle left items**). The initial WTD controls which soil layers are affected by drainage, which is in turn related to the amount and lability (active, slow, passive) of SOC exposed to oxygen, thereby influencing the sensitivities.

Finally, air temperature was also found to have a correlation with sensitivities. Sites in warmer climates tend to have more sensitive NEE ($R^2 = 0.73$, $p = 0.002$) and CH_4 emission ($R^2 = 0.86$, $p < 0.001$) responses (**Figure 9 a and b, middle right items**). However, it remains uncertain whether these correlations are causal or reflect co-variations between temperature and other factors, given the small number of points in the regressions shown in **Fig. 9**.

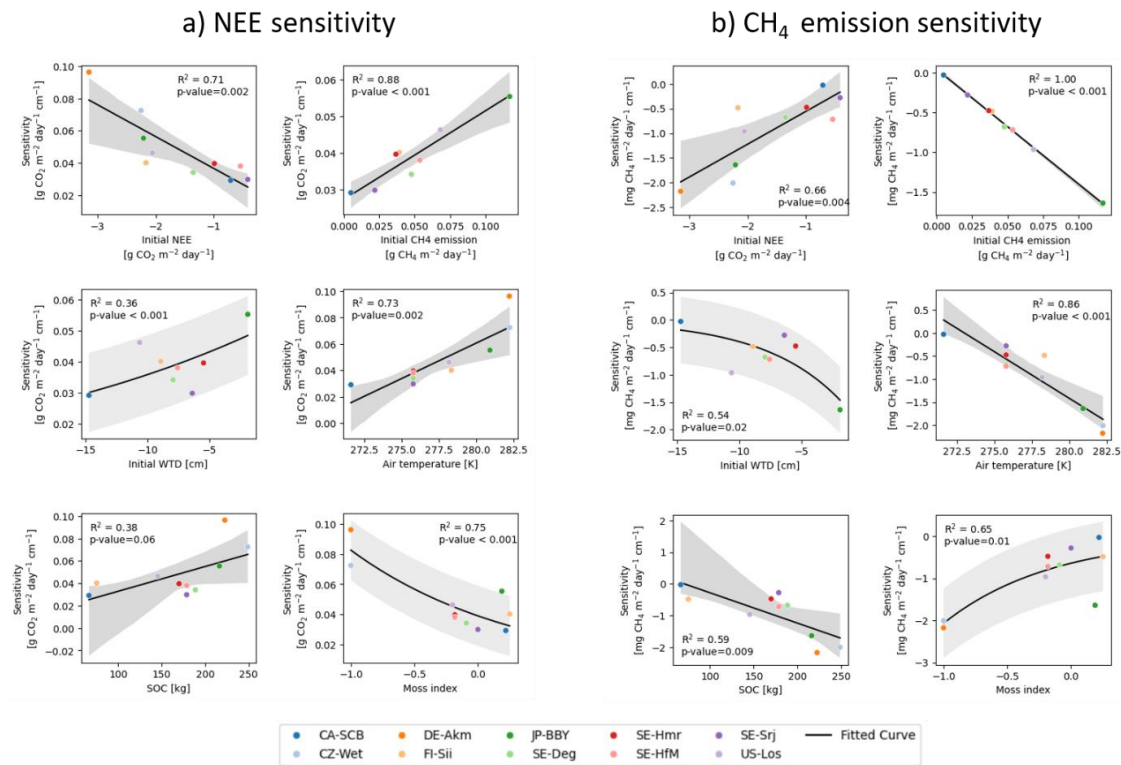


Figure 9. Relationships between the sensitivities of (a) net ecosystem exchange (NEE) and (b) CH_4 emissions to water table drawdown and selected site-level variables, including initial NEE, initial CH_4 emissions, initial water table depth (WTD), air temperature, soil organic carbon content (SOC), and the moss index (MI). Solid lines show fitted regression relationships across sites, and gray shaded areas indicate the 95% confidence interval of the fitted regression. The moss index represents the relative cover fraction of mosses compared to vascular plants. The analysis is based on modeled results from the first 10 years of drainage simulations.

3.7 Building an exploratory emulator of sensitivities for GHG accounting and decision support applications.

It is impractical to run a complex, process-calibrated model like ORCHIDEE-PEAT for calculating the sensitivities of GHG fluxes to drainage over a whole region, for instance, to derive spatially variables emission factors that could be used in GHG accounting studies (IPCC Guidelines Tier 3, Eggleston, (2006)) and decision support tools or meta-models like (e.g. FAO, 2021). Therefore, following the analysis of the driving factors of the sensitivities in the previous section (Fig. 9), we developed an emulator of the model sensitivities based on multilinear regressions. Given the limited number of sites and the acknowledged limitations of the underlying process-based model, the emulator presented here is intended as an exploratory, proof-of-concept approach rather than a fully validated predictive tool. To do so, we first fitted all possible regressions of the simulated sensitivities (S_{NEE} and S_{CH4}) against the six variables as shown in Fig 9, including initial NEE (NEE_{init}), initial CH₄ emission ($CH4_{init}$), initial water table (WTD_{init} in cm), soil organic carbon content (SOC in kgC/m²), air temperature (T in K), and moss index (MI). Then, the best regression model was selected based on the minimum corrected Akaike information criterion (AICc, Appendix C), constrained by the cutoff of variance inflation factor (VIF) > 5 to avoid multicollinearity among predictors (Fig. C4):

$$S_{NEE} = 0.022 - 0.013 \times NEE_{init} - 0.025 \times MI \quad (R^2 = 0.91, p \leq 0.001) \quad (3)$$

$$S_{CH4} = 0.045 - 14.426 \times CH4_{init} \quad (R^2 = 0.998, p \leq 0.001) \quad (4)$$

To evaluate the robustness of the selected model, a leave-one-out cross-validation was performed. The model was re-fitted multiple times, each time excluding one site from the data, and the performance metrics (R^2 and p-value) were recorded for the withheld site (Table C1). The small variation in R^2 (+std of R^2) and p-value (+std of p-value) among all re-fitted models suggests that the selected regression relationships are internally consistent across sites, within the limits of the available sample.

Furthermore, we calculated the product of the regression coefficients for each variable in Equation (3) by their standard deviations between sites to quantify the ‘effect’ of each variable on the sensitivity (Jung et al., 2017). For the sensitivity of NEE, the effect of NEE_{init} is -0.012, comparable to that of MI , at -0.011.

3.8 Combined effect of CO₂ and CH₄ changes

To assess the combined climate forcing of CO₂ and CH₄ flux changes due to drainage, we used the Global Warming Potential (GWP) metric to convert methane emissions into CO₂-equivalents (IPCC AR6). **Figure 10** shows the resulting CO₂-equivalent flux changes averaged across the 10 sites for 20- and 50-year periods of drainage as a function of the WTD drawdown. We used GWP100 = 27 for the 50-year period and GWP20 = 79.7 (IPCC, 2023) shown in different colors in **Figure 10**. At the site scale, the simulated CO₂-equivalent flux changes exhibit substantial uncertainty, as reflected by the error bars in **Fig. 10**. These uncertainties arise from both parameter uncertainty and uncertainty associated with vegetation cover changes induced by drainage, the latter quantified as the range across alternative vegetation scenarios explored in **Appendix D**.

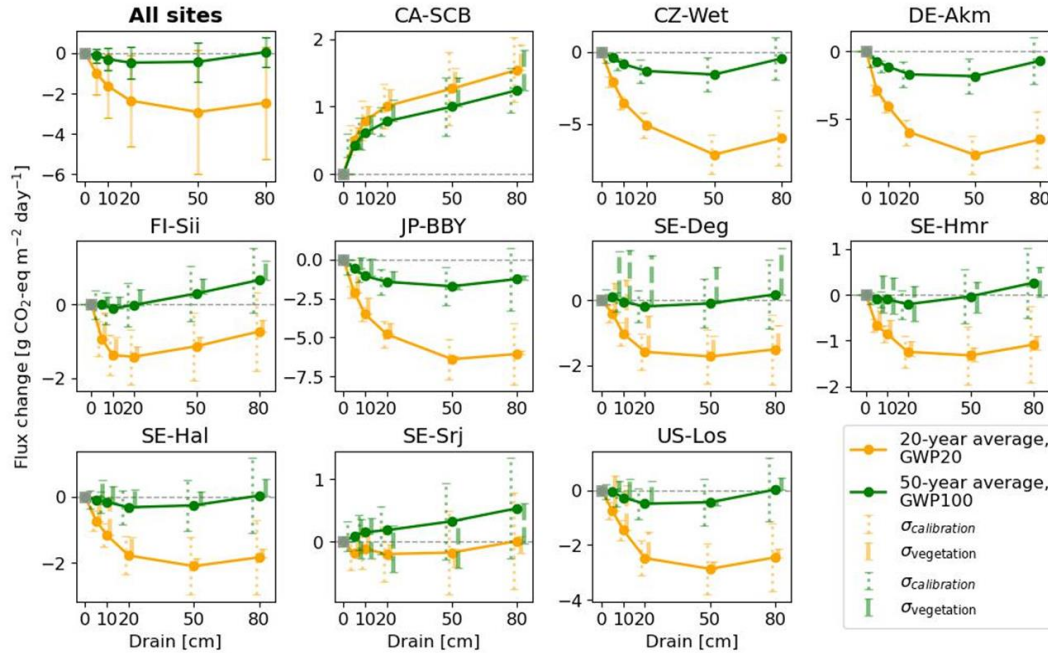


Figure 10. Change in fluxes (relative to undrained) expressed as CO₂-equivalents by drainage level (x-axis), averaged over 20 and 50 years following the start of drainage. CH₄ emissions were converted to CO₂-equivalents using GWP20 for 20-year average (orange lines) and GWP100 for the 50-year average (green line). In the plot with all sites, the error bars parameter calibration uncertainty ($\sigma_{\text{calibration}}$), quantified as ± 1 standard deviation of the simulated time-mean CO₂-equivalent fluxes over the full 50-year simulation period across 10 Monte Carlo runs, and vegetation

scenario uncertainty ($\sigma_{\text{vegetation}}$), defined as the minimum–maximum range of simulated responses across alternative vegetation change scenarios (see **Appendix D**).

645

Averaging our model results for all 10 sites at 80-cm drainage leads to a slight warming of 0.05 g CO₂-eq m⁻² day⁻¹ using GWP100 after 50 years of drainage, and to a cooling of -2.46 g CO₂-eq m⁻² day⁻¹ using GWP20 after 20 years. In comparison, from the data collected by meta-analysis studies (Huang et al., 2021b; Zou et al., 2022), retaining only sites where both ΔNEE and ΔCH_4 flux are available, we calculated for all sites a mean cooling effect of -5.46 g CO₂-eq m⁻² day⁻¹ with a huge spread (95% CI: -73.06 to 17.64) using GWP20, and a mean cooling of -0.06 g CO₂-eq m⁻² day⁻¹ (-25.60 to 11.82) using GWP100, with the occurrence of cooling and warming effects being almost equal among all the sites (**Fig. C5**). This result is rather consistent with our model simulations. In contrast, pooling all sites and WTD levels together, thus combining ΔCO_2 and ΔCH_4 from different locations in an inconsistent manner, from the data of Zou et al. (2022) excluding their reported N₂O emissions changes, a net cooling effect of -0.30 g CO₂-eq m⁻² day⁻¹ using GWP100 was estimated. Similarly, using a GWP100 value of 25, Huang et al. (2021b) estimated across their sites a net warming effect of 0.033 g CO₂-eq m⁻² h⁻¹ (0.009 to 0.057). This suggests that the averaging of sites from meta-analysis data can lead to assessing either a cooling or a warming, depending on whether only sites with both measured ΔCO_2 and ΔCH_4 are used, or all sites are used.

Our model simulations also show that different drainage periods and the choice of a different GWP time horizons lead to distinct warming or cooling effects (**Fig. 10**). For 9 sites out of 10 (i.e. except CA-SCB), however, we simulated a larger cooling on a 20-year horizon compared to a 100-year horizon, due to the stronger radiative forcing impact of reduced CH₄ emissions in the short term. In addition, most of the sites show a larger radiative forcing change when the WTD is deeper, specifically a higher cooling from reduced CH₄ emissions on a 20-year horizon. Secondly, the magnitude and the sign of changes, whether warming or cooling, varies significantly between sites. CA-SCB is the only site having warming effects (from 0.4 to 1.5 g CO₂-eq m⁻² day⁻¹) regardless of time scales and drainage levels. On the other hand, CZ-Wet, DE-Akm, JP-BBY always have cooling effects (down to -6.5 g CO₂-eq m⁻² day⁻¹) because their CH₄ emissions are reduced more than their CO₂ emissions are increased. Other sites have both warming and cooling effects depending on time scale considered and drainage level. Neutral effects on climate were observed in some cases,

670

primarily when considering 50 years of drainage (green line), such as FI-Sii with a 20 cm drainage and US-Los at a 80 cm drainage level.

675 **4 Discussion**

Uncertainty in our simulations involves several factors, typically coming from model calibration, our WTD reconstruction, and the omission of vegetation change during drainage and possible changes of soil structure including compaction. Our model represents an advance compared to the state of the art but remains limited in its ability to mechanistically represent drained peatland systems, particularly regarding extrapolation and representation of dynamic soil and hydrological processes. Some of the limitations are discussed below and raise caution in interpreting model outputs as representative of real-world conditions.

680 Firstly, two sites could not be calibrated with CH₄ emission but only with NEE, due to a lack of CH₄ measurements. A good simulation of methane processes is expected to improve CO₂ emissions because the oxidation of methane in soil produces CO₂ which contributes to the total NEE (CO₂ from methanotrophy constitutes 8.21% (95% CI: 0.57% - 29.81%) of heterotrophic respiration). For sites without CH₄ calibration, CH₄ parameters were currently taken from the average of calibrated parameters of other sites. Another solution that could be tried is to do multi-site calibration of CH₄ and NEE for the sites with both observations where they are available, i.e. 690 optimize a single set of parameters that best compromises between all sites, then take the resulting CH₄ parameters for the sites that are not CH₄-calibrated. Anyway, uncertainties still remain, as climate and environmental conditions vary between sites. Liu et al. (2025) showed that even multi-site calibration sometimes cannot significantly improve the performance of the model due to the inability of the model to consider all trait-climate correlations, with constant parameters used for 695 traits instead.

Secondly, although we believe that our method to reconstruct WTD from soil moisture using a machine learning (ML) module is an interesting and viable solution for now, the training of a ML model to derive a function from few sites which is then applied to other sites where WTD is missing could be problematic if extrapolation is required out of the training range. We assumed that all

700 peatland sites in this study share the same relationship between soil moisture and water table. However, peatlands in different locations can have different peat soil characteristics, along with varying environmental, terrain, and water supply conditions, so the assumption can inevitably be wrong in some places. One thing we can expect in the future is that when we have more water table data everywhere, this indirect reconstruction of WTD can work better.

705 Thirdly, changes in vegetation cover on peat soil caused by drainage have not been considered in this study due to the complexity of processes and lack of long term data. With water table drawdown and subsequent physical and chemical alterations, peat soils can become more favorable for certain plants (e.g., vascular plants) and less favorable for others (e.g., some *Sphagnum* mosses), potentially resulting in a shift in vegetation composition (Antala et al., 2022; Kokkonen et al., 2022).
710 Peatland specialist species adapted to waterlogged conditions may even disappear after water table drawdown (Jassey et al., 2018), while woody species can invade newly available growing spaces (Kokkonen et al., 2019). Additionally, species turnover also depends on the type of peatland (e.g. bog/fen), particularly on hydrological and nutrient conditions prior to drainage (Kokkonen et al., 2022). Changes in plant composition should be incorporated into drainage simulations, as each PFT
715 has unique photosynthetic capacity, respiration rates, and contributes litter of varying quality for decomposition, all of which would impact the carbon balance and CH₄ emission. While it's straightforward to introduce in a model a new vegetation composition, simulating the dynamic changes in vegetation - such as determining the factors controlling moss disappearance and adjusting PFT fractions accordingly - remains challenging. Similarly, the model parameters, which
720 were calibrated based on undisturbed fluxes, remained unchanged during the simulation of drainage scenarios, even though soil hydrological parameters such as water holding capacity and water conductivity are known to be affected by compaction during drainage. In order to address this limitation, to explore the potential impact of vegetation shifts, we conducted a sensitivity test with alternative peatland PFT compositions (**Appendix D**). The results show that vegetation shifts can
725 indeed influence the net effect of drainage on GHG emissions: in some cases, it amplified the warming effect, while in others, it reversed a cooling effect into a net warming, or vice versa.

In the ditch drainage simulation, we assumed an ideal condition in which the drained peatland is effectively isolated from adjoining land and suppressed the runoff from other soil tiles to the peat

soil tile. This is not always what happens in reality, there can still be runoff entering the peatland
730 from adjoining land. However, this suppression helps to make the peat soil effectively dried in the
model. With the limitation in representing the drainage complexity, the ditch drains water from the
peat soil tile only, and not from other soil tiles. The runoff from other soil tiles to the peat soil tile
that is suppressed in the model can be interpreted as accounting for the horizontal water flow from
these tiles that should have also been drained by the ditch. We also assumed a uniform water table
735 drawdown across the whole peatland and over the course of 50 years. However, in reality, the water
table near the ditch can differ significantly from microscale effects, or to some extent, from the
water table farther away from it. This depends on the hydraulic conductivity of peat materials, which
varies with the degree of peat decomposition (Boelter, 1972). Also, a peatland over time may often
recover back to the same water table depth after drainage, because subsidence and oxidation will
740 bring the surface down close to the previous water table level (Hilbert et al., 2000; Waddington et
al., 2015). Considering distance to ditch and subsidence effects would help move towards a more
realistic simulation.

In the analysis of emission factors (EF), we explained their variation by a few processes related
to litter and SOC. There are also other factors that can affect the change of EF by time (whether
745 increasing or decreasing) but were not simulated or considered in the analysis. For example, peat
bulk density and porosity can alter due to drainage. Investigating their behaviors could provide
better insights into EF variations. A key limitation is that in the current ORCHIDEE model, certain
soil characteristics (e.g. peat bulk density and porosity) are treated as constant. In field experiments,
it was found that highly decomposed peat due to drainage can be more vulnerable to further
750 breakdown by microbial decomposition (Säurich et al., 2019), which is influenced by both peat
properties and nutrient status. Yet, our current model does not explicitly track the progressive
degradation of individual SOC components or incorporate nutrient feedbacks to diagnose their
corresponding reactivity. Decomposition could be calculated based only on fixed residence times
for three carbon pools, which is a parameter calibrated under pre-drained conditions. Simulating
755 peat properties and their feedbacks as dynamic variables would require further model development,
for instance, adjusting over time the turnover times of carbon pools to simulate more realistic
decomposition conditions.

We also need in future studies to take into account the emission of CH₄ that is dissolved in water drained out, produced in-situ in the ditch, and diffused at the vertical cross-section surface of the ditch. According to Roulet and Moore (1995), a drainage ditch is a direct source of methane because (1) evacuated water transports CH₄ from the surrounding peat into the ditch, and (2) CH₄ production is favorable in the ditch where sediment is constantly saturated and warmed by direct solar radiation. Recent studies based on meta-analysis report an offset of drainage ditch to the methane reduction due to drainage, which is 18% by Peacock et al. (2021), 12 (10-14) % by Gan et al. (2024). Roulet and Moore (1995) suggested that flow rate, depth, and morphology of the ditch can have an impact on its CH₄ emission, and ditch spacing also plays a role in net CH₄ emission of the landscape.

Finally, in our simulation protocol, the present climate conditions are recirculated over the whole time of future simulation in so-called idealized scenarios, but it is interesting for future studies to use climate conditions predicted for the future using climate change scenarios, for instance, with the Inter-Sectoral Impact Model Intercomparison Project (ISIMIP) database (Lange and Büchner, 2021). Using future climate forcing is simple, but then we will also need a corresponding forecast of climate induced future WTD changes for the baseline scenario, and here again our machine-learning model to compute undisturbed WTD from modeled soil moisture may not work for unseen future soil moisture conditions.

Despite these limitations, an independent comparison with field observations from a long-term drainage experiment conducted at a site near FI-Sii shows that the model reproduces the observed increase in ecosystem respiration and reduction in CH₄ emissions under drained conditions reasonably well (**Appendix E; Fig. E1**). This comparison provides additional support that, within the limits discussed above, the model is able to capture key aspects of drainage-induced greenhouse gas flux responses under real-world conditions.

Overall, building on the results and limitations discussed above, this study demonstrates that implementing a peatland drainage module within a land surface model is feasible and yields physically consistent responses of CO₂ and CH₄ fluxes to water table drawdown across contrasting sites. At the same time, the results highlight key structural and process-level challenges that remain

to be addressed, including dynamic vegetation shifts, evolving peat physical properties, lateral water and carbon fluxes, and improved representation of long-term post-drainage processes. Addressing these challenges represents a clear priority for future model development before such a framework can be applied for robust large-scale predictive assessments.

790 **5 Conclusions**

In this study, we addressed the difficult problem of estimating changes of CO₂ and CH₄ fluxes when peatlands are drained in the future. Insofar, most of the knowledge comes from empirical results that showed a general increase of CO₂ emissions and a decrease of CH₄ emissions during drainage. Yet, meta-analysis data group fluxes from different experiments, where CO₂ and CH₄ fluxes are not always measured simultaneously, and include different control conditions, thus showing a large spread of their results. We used a process model calibrated to match fluxes under pristine conditions before drainage from 10 sites individually and parameterized virtual drainage at each site with a new ditch module. The model was integrated forward for virtual drainage simulations at each site under the present climate with different prescribed water table depths. A summary of the answers to the research questions posed in the introduction is given below.

(1) What are the changes of CO₂ and CH₄ fluxes in response to drainage and how do they compare with observations? We found an increase of CO₂ emissions or a decrease of CO₂ sinks and a decrease of CH₄ emissions from drainage, with a magnitude very similar to the observations in flux data collected by Evans et al. (2021) and within the range of meta-analysis results, although meta-analysis results have a huge variability. On average, we predict for the first decade of 50 cm drainage a reduction of the CO₂ sink of 3.14 g CO₂ m⁻² day⁻¹ (0.23 to 10.97) and a decrease of CH₄ emissions of -0.06 g CH₄ m⁻² day⁻¹ (-0.21 to 0.001).

(2) How do fluxes change as a function of drainage duration? We found that a longer drainage period leads to a diminishment of the increase of CO₂ emissions, and to a strengthening of the CH₄ emission reduction over time with longer drainage. The first result for CO₂ is consistent with previous emission factors simulated for peat drained to croplands agriculture (Qiu et al., 2021). Such a model as presented here, if validated against real-world observations, can help provide time-

dependent emission factors that may be useful for inventory calculations in the absence of long-term CH₄ emission factor changes from measurements. It should be emphasized that model evaluation against observations is currently limited to the first decade following drainage, and that simulated changes over longer drainage durations represent model-based extrapolations that should be interpreted as exploratory scenarios rather than validated predictions.

(3) What is the modeled sensitivity of flux changes to water table depth? We found that the shallower the starting water table, the more positive the sensitivity of CO₂ flux changes to WTD (more warming) and the greater is the sensitivity of CH₄ reductions (more cooling from suppressed CH₄ emissions).

(4) What factors affect the sensitivity at each site in the model? We found that, in the model world, the initial fluxes, initial water table depth, soil organic carbon, moss fraction and temperature are the key influential factors controlling the sensitivities across sites. These variables have strong covariations in the model, so their effect cannot be isolated individually. The emulator is constructed from sensitivities of modeled GHG fluxes to water table depth derived from the first 10 years following drainage, corresponding to the period over which the model has been evaluated against observations. This finding allowed us to propose an emulator of the modeled sensitivities that could be used to predict flux changes at other sites or over a region. Yet, this is only a model result and testing it against observations would be important in the future to use such an emulator approach for GHG accounting.

(5) What is the net climate effect of CO₂ and CH₄ flux changes induced by drainage using the GWP metrics to compare CH₄ with CO₂. Here we found that, averaged over all WTD depths, drainage during 20 years with radiative forcing calculated with GWP20 is projected by our model to induce a net cooling because the reduction of CH₄ emissions dominates over changes of CO₂ fluxes. Drainage during 50 years with GWP100 induces almost a net neutral effect. There is a large variability between sites even for the sign of the climate effect of drainage. This gives a more nuanced perspective than the current paradigm that drainage always warms the climate. Importantly, uncertainty in future vegetation, as illustrated by the sensitivity analysis in **Appendix D**, is not a minor sensitivity: different plausible vegetation scenarios can qualitatively change the assessed

climate impact of drainage, including reversing the sign of the net climate effect, and therefore directly affect the interpretation of these results. However, our prediction of a net cooling using GWP20 differs from most previous meta-analysis results and should be interpreted with caution, because it relies on model-based projections extending well beyond the 20-year time horizon
845 associated with the use of GWP20. This result seems at first glance opposite to meta-analysis results, even though our model simulations for flux changes were found to be consistent with these data. The data do not have very long drainage experiments, which may explain the differences with our predictions. However, when taking only sites from meta-analysis studies where both CO₂ and CH₄ fluxes changes were measured, a net cooling is found, consistent with our model-based projections.

850 Finally, although our study explicitly quantified uncertainties arising from parameter calibration and alternative vegetation trajectories, there remain ‘known unknown’ uncertainties associated with potential future parameter shifts and unresolved model structural limitations. These include changes in organic matter decomposition induced by reduced phenolic compounds during dry conditions (as phenols normally inhibit microbial activity and therefore prevent the breakdown
855 of organic matter) (Fenner and Freeman, 2011), shifts in the molecular composition and stability of soil organic carbon from microbe-, plant- and re-derived sources in response to drainage-induced soil warming and future elevated CO₂ (Ofiti et al., 2023), and the suppression of dissolved organic carbon export during drainage (Rosset et al., 2022).

Future work should consider additional CH₄ emissions from ditch water and shifts of
860 vegetation composition during drainage. Furthermore, our results show that vegetation shifts represent a major source of systematic uncertainty in our predictions, and that different plausible future vegetation trajectories can reverse the sign of the simulated climate effects, thereby directly affecting the interpretation of our conclusions on net climate impacts. This model framework can be applied for regional historical simulations to improve on previous studies where drainage was
865 not explicitly modeled but represented as an abrupt land cover change from peat to cropland, and where CH₄ effects were ignored. It can also be applied to future rewetting scenarios of degraded peat to assess the net climate effect of this nature based solution.

Author contribution

PC – Conceptualization. THN and LL– Methodology, simulations, and formal analysis. YX, CQ,
870 and ES contributed to simulations. AK, CG, MP, JR, KDN, and XL provided site data. PC and THN
wrote the manuscript, PC and LL revised the manuscript, all co-authors reviewed and edited it.

Acknowledgements

This research was carried out in the framework of the European Union’s Horizon Europe
programme WET HORIZONS, grant agreement no. 101056848. E. Salmon is funded by the
875 European Union's Horizon research and innovation program, HORIZON-CL5-2021-D1-01,
GreenFeedback under grant agreement no. 101056921.

References

- 880 Akaike, H.: A new look at the statistical model identification, *IEEE Transactions on Automatic
Control*, 19, 716–723, <https://doi.org/10.1109/TAC.1974.1100705>, 1974.
- Antala, M., Juszczak, R., Van Der Tol, C., and Rastogi, A.: Impact of climate change-induced
alterations in peatland vegetation phenology and composition on carbon balance, *Science of
The Total Environment*, 827, 154294, <https://doi.org/10.1016/j.scitotenv.2022.154294>, 2022.
- 885 Arnold, K. V., Weslien, P., Nilsson, M., Svensson, B. H., and Klemedtsson, L.: Fluxes of CO₂,
CH₄ and N₂O from drained coniferous forests on organic soils, *Forest Ecology and
Management*, 210, 239–254, <https://doi.org/10.1016/j.foreco.2005.02.031>, 2005.
- Aurela, M., Riutta, T., Laurila, T., Tuovinen, J.-P., Vesala, T., Tuittila, E.-S., Rinne, J., Haapanala,
S., and Laine, J.: CO₂ exchange of a sedge fen in southern Finland—the impact of a drought
890 period, *Tellus B: Chemical and Physical Meteorology*, 59, 826, [https://doi.org/10.1111/j.1600-
0889.2007.00309.x](https://doi.org/10.1111/j.1600-
0889.2007.00309.x), 2007.
- Bernhofer, C., Grünwald, T., Moderow, U., Hehn, M., Eichelmann, U., Prasse, H., and Postel, U.:
FLUXNET2015 DE-Akm Anklam, <https://doi.org/10.18140/FLX/1440213>, 2009.

- Blodau, C.: Carbon cycling in peatlands A review of processes and controls, *Environ. Rev.*, 10, 895 111–134, <https://doi.org/10.1139/a02-004>, 2002.
- Boelter, D. H.: Water table drawdown around an open ditch in organic soils, *Journal of Hydrology*, 15, 329–340, [https://doi.org/10.1016/0022-1694\(72\)90046-7](https://doi.org/10.1016/0022-1694(72)90046-7), 1972.
- Conchedda, G. and Tubiello, F. N.: Drainage of organic soils and GHG emissions: validation with country data, *Earth Syst. Sci. Data*, 12, 3113–3137, <https://doi.org/10.5194/essd-12-3113-2020>, 900 2020.
- Couwenberg, J., Dommain, R., and Joosten, H.: Greenhouse gas fluxes from tropical peatlands in south-east Asia, *Global Change Biology*, 16, 1715–1732, <https://doi.org/10.1111/j.1365-2486.2009.02016.x>, 2010.
- Desai, A. and Thom, J.: FLUXNET-CH4 US-Los Lost Creek, 905 <https://doi.org/10.18140/FLX/1669682>, 2020.
- Ducharne, A., Ottlé, C., Maignan, F., Vuichard, N., Ghattas, J., Wang, F., Peylin, P., Polcher, J., Guimberteau, M., Maugis, P., Tafasca, S., Tootchi, A., Verhoef, A., and Mizuochi, H.: The hydrol module of ORCHIDEE: scientific documentation [ref 3977 and on], work in progress, towards CMIP6v1, 2018.
- 910 Eggleston, H. S. (Ed.): 2006 IPCC guidelines for national greenhouse gas inventories, Institute for Global Environmental Strategies, Hayama, Japan, 2006.
- Evans, C. D., Peacock, M., Baird, A. J., Artz, R. R. E., Burden, A., Callaghan, N., Chapman, P. J., Cooper, H. M., Coyle, M., Craig, E., Cumming, A., Dixon, S., Gauci, V., Grayson, R. P., Helfter, C., Heppell, C. M., Holden, J., Jones, D. L., Kaduk, J., Levy, P., Matthews, R., 915 McNamara, N. P., Misselbrook, T., Oakley, S., Page, S. E., Rayment, M., Ridley, L. M., Stanley, K. M., Williamson, J. L., Worrall, F., and Morrison, R.: Overriding water table control on managed peatland greenhouse gas emissions, *Nature*, 593, 548–552, <https://doi.org/10.1038/s41586-021-03523-1>, 2021.
- FAO: Peat-GHG tool: A greenhouse gas calculator for peatland management in Indonesia, 2021.
- 920 Fenner, N. and Freeman, C.: Drought-induced carbon loss in peatlands, *Nature Geosci*, 4, 895–900, <https://doi.org/10.1038/ngeo1323>, 2011.

- Friedlingstein, P., O’Sullivan, M., Jones, M. W., Andrew, R. M., Gregor, L., Hauck, J., Le Quéré, C., Luijkx, I. T., Olsen, A., Peters, G. P., Peters, W., Pongratz, J., Schwingshackl, C., Sitch, S., Canadell, J. G., Ciais, P., Jackson, R. B., Alin, S. R., Alkama, R., Arneeth, A., Arora, V. K.,
925 Bates, N. R., Becker, M., Bellouin, N., Bittig, H. C., Bopp, L., Chevallier, F., Chini, L. P., Cronin, M., Evans, W., Falk, S., Feely, R. A., Gasser, T., Gehlen, M., Gkritzalis, T., Gloege, L., Grassi, G., Gruber, N., Gürses, Ö., Harris, I., Hefner, M., Houghton, R. A., Hurtt, G. C., Iida, Y., Ilyina, T., Jain, A. K., Jersild, A., Kadono, K., Kato, E., Kennedy, D., Klein Goldewijk, K., Knauer, J., Korsbakken, J. I., Landschützer, P., Lefèvre, N., Lindsay, K., Liu, J., Liu, Z.,
930 Marland, G., Mayot, N., McGrath, M. J., Metz, N., Monacchi, N. M., Munro, D. R., Nakaoka, S.-I., Niwa, Y., O’Brien, K., Ono, T., Palmer, P. I., Pan, N., Pierrot, D., Pockock, K., Poulter, B., Resplandy, L., Robertson, E., Rödenbeck, C., Rodriguez, C., Rosan, T. M., Schwinger, J., Séférian, R., Shutler, J. D., Skjelvan, I., Steinhoff, T., Sun, Q., Sutton, A. J., Sweeney, C., Takao, S., Tanhua, T., Tans, P. P., Tian, X., Tian, H., Tilbrook, B., Tsujino, H., Tubiello, F.,
935 van der Werf, G. R., Walker, A. P., Wanninkhof, R., Whitehead, C., Willstrand Wranne, A., et al.: Global Carbon Budget 2022, *Earth System Science Data*, 14, 4811–4900, <https://doi.org/10.5194/essd-14-4811-2022>, 2022.
- Furukawa, Y., Inubushi, K., Ali, M., Itang, A. M., and Tsuruta, H.: Effect of changing groundwater levels caused by land-use changes on greenhouse gas fluxes from tropical peat lands, *Nutr Cycl Agroecosyst*, 71, 81–91, <https://doi.org/10.1007/s10705-004-5286-5>, 2005.
940
- Gan, D., Zhang, Z., Li, H., Yu, D., Li, Z., Long, R., Niu, S., Zuo, H., Meng, X., Wang, J., and Ma, L.: Ditch emissions partially offset global reductions in methane emissions from peatland drainage, *Commun Earth Environ*, 5, 640, <https://doi.org/10.1038/s43247-024-01818-5>, 2024.
- Hilbert, D. W., Roulet, N., and Moore, T.: Modelling and analysis of peatlands as dynamical systems, *Journal of Ecology*, 88, 230–242, <https://doi.org/10.1046/j.1365-2745.2000.00438.x>, 2000.
945
- Holden, J.: Peatland hydrology and carbon release: why small-scale process matters, *Phil. Trans. R. Soc. A.*, 363, 2891–2913, <https://doi.org/10.1098/rsta.2005.1671>, 2005.
- Huang, X., Silvennoinen, H., Kløve, B., Regina, K., Kandel, T. P., Piayda, A., Karki, S., Lærke, P. E., and Höglind, M.: Modelling CO₂ and CH₄ emissions from drained peatlands with grass

- 950 cultivation by the BASGRA-BGC model, *Science of The Total Environment*, 765, 144385,
<https://doi.org/10.1016/j.scitotenv.2020.144385>, 2021a.
- Huang, Y., Ciais, P., Luo, Y., Zhu, D., Wang, Y., Qiu, C., Goll, D. S., Guenet, B., Makowski, D.,
De Graaf, I., Leifeld, J., Kwon, M. J., Hu, J., and Qu, L.: Tradeoff of CO₂ and CH₄ emissions
from global peatlands under water-table drawdown, *Nat. Clim. Chang.*, 11, 618–622,
955 <https://doi.org/10.1038/s41558-021-01059-w>, 2021b.
- Intergovernmental Panel On Climate Change (IPCC): *Climate Change 2021 – The Physical Science
Basis: Working Group I Contribution to the Sixth Assessment Report of the Intergovernmental
Panel on Climate Change*, 1st ed., Cambridge University Press,
<https://doi.org/10.1017/9781009157896>, 2023.
- 960 Jassey, V. E. J., Reczuga, M. K., Ziełńska, M., Słowińska, S., Robroek, B. J. M., Mariotte, P.,
Seppey, C. V. W., Lara, E., Barabach, J., Słowiński, M., Bragazza, L., Chojnicki, B. H.,
Lamentowicz, M., Mitchell, E. A. D., and Buttler, A.: Tipping point in plant–fungal
interactions under severe drought causes abrupt rise in peatland ecosystem respiration, *Global
Change Biology*, 24, 972–986, <https://doi.org/10.1111/gcb.13928>, 2018.
- 965 Joosten, H.: *The Global Peatland CO₂ Picture: peatland status and drainage related emissions in all
countries of the world*, 2009.
- Jung, M., Reichstein, M., Schwalm, C. R., Huntingford, C., Sitch, S., Ahlström, A., Arneeth, A.,
Camps-Valls, G., Ciais, P., Friedlingstein, P., Gans, F., Ichii, K., Jain, A. K., Kato, E., Papale,
D., Poulter, B., Raduly, B., Rödenbeck, C., Tramontana, G., Viovy, N., Wang, Y.-P., Weber,
970 U., Zaehle, S., and Zeng, N.: Compensatory water effects link yearly global land CO₂ sink
changes to temperature, *Nature*, 541, 516–520, <https://doi.org/10.1038/nature20780>, 2017.
- Kiew, F., Hirata, R., Hirano, T., Xhuan, W. G., Aries, E. B., Kemudang, K., Wenceslaus, J., San, L.
K., and Melling, L.: Carbon dioxide balance of an oil palm plantation established on tropical
peat, *Agricultural and Forest Meteorology*, 295, 108189,
975 <https://doi.org/10.1016/j.agrformet.2020.108189>, 2020.
- Kokkonen, N., Laine, A. M., Laine, J., Vasander, H., Kurki, K., Gong, J., and Tuittila, E.: Responses
of peatland vegetation to 15-year water level drawdown as mediated by fertility level, *J
Vegetation Science*, 30, 1206–1216, <https://doi.org/10.1111/jvs.12794>, 2019.

- 980 Kokkonen, N., Laine, A. M., Männistö, E., Mehtätalo, L., Korrensalo, A., and Tuittila, E.-S.: Two Mechanisms Drive Changes in Boreal Peatland Photosynthesis Following Long-Term Water Level Drawdown: Species Turnover and Altered Photosynthetic Capacity, *Ecosystems*, 25, 1601–1618, <https://doi.org/10.1007/s10021-021-00736-3>, 2022.
- Kwon, M. J., Ballantyne, A., Ciais, P., Qiu, C., Salmon, E., Raoult, N., Guenet, B., Göckede, M., Euskirchen, E. S., Nykänen, H., Schuur, E. A. G., Turetsky, M. R., Dieleman, C. M., Kane, E. S., and Zona, D.: Lowering water table reduces carbon sink strength and carbon stocks in northern peatlands, *Global Change Biology*, 28, 6752–6770, <https://doi.org/10.1111/gcb.16394>, 2022.
- Laine, A. M., Byrne, K. A., Kiely, G., and Tuittila, E.-S.: carbon dioxide and methane fluxes in a blanket bog, 2009.
- 990 Lange, S. and Büchner, M.: ISIMIP3b bias-adjusted atmospheric climate input data (1.1), <https://doi.org/10.48364/ISIMIP.842396.1>, 2021.
- Larmola, T., Tuittila, E.-S., Tirola, M., Nykänen, H., Martikainen, P. J., Yrjälä, K., Tuomivirta, T., and Fritze, H.: The role of Sphagnum mosses in the methane cycling of a boreal mire, *Ecology*, 91, 2356–2365, <https://doi.org/10.1890/09-1343.1>, 2010.
- 995 Liu, L., Qiu, C., Xi, Y., Salmon, E., Kalhori, A., Artz, R. R. E., Guimbaud, C., Peichl, M., Ratcliffe, J. L., Noumonvi, K. D., López, E., Dusek, J., Markkanen, T., Sachs, T., Aurela, M., Nguyen, T.-H., Lohila, A., Mammarella, I., and Ciais, P.: Assessing CO₂ Fluxes for European Peatlands in ORCHIDEE-PEAT With Multiple Plant Functional Types, *Journal of Advances in Modeling Earth Systems*, 17, <https://doi.org/10.1029/2025MS004940>, 2025.
- 1000 Lynch, J., Cain, M., Pierrehumbert, R., and Allen, M.: Demonstrating GWP*: a means of reporting warming-equivalent emissions that captures the contrasting impacts of short- and long-lived climate pollutants, *Environ. Res. Lett.*, 15, 044023, <https://doi.org/10.1088/1748-9326/ab6d7e>, 2020.
- Maljanen, M., Sigurdsson, B. D., Guðmundsson, J., Óskarsson, H., Huttunen, J. T., and Martikainen, P. J.: Greenhouse gas balances of managed peatlands in the Nordic countries – present knowledge and gaps, *Biogeosciences*, 7, 2711–2738, <https://doi.org/10.5194/bg-7-2711-2010>, 2010.
- 1005

- 1010 Martikainen, P. J., Nykänen, H., Alm, J., and Silvola, J.: Change in fluxes of carbon dioxide, methane and nitrous oxide due to forest drainage of mire sites of different trophic, *Plant Soil*, 168–169, 571–577, <https://doi.org/10.1007/BF00029370>, 1995.
- Mejdová, M., Dušek, J., Foltýnová, L., Macálková, L., and Čížková, H.: Photosynthetic parameters of a sedge-grass marsh as a big-leaf: effect of plant species composition, *Sci Rep*, 11, 3723, <https://doi.org/10.1038/s41598-021-82382-2>, 2021.
- 1015 Mohammed Rashid, A., Midi, H., Dhhan, W., and Arasan, J.: Detection of outliers in high-dimensional data using *nu* -support vector regression, *Journal of Applied Statistics*, 49, 2550–2569, <https://doi.org/10.1080/02664763.2021.1911965>, 2022.
- Mozafari, B., Bruen, M., Donohue, S., Renou-Wilson, F., and O’Loughlin, F.: Peatland dynamics: A review of process-based models and approaches, *Science of The Total Environment*, 877, 162890, <https://doi.org/10.1016/j.scitotenv.2023.162890>, 2023.
- 1020 Munir, T. M., Perkins, M., Kaing, E., and Strack, M.: Carbon dioxide flux and net primary production of a boreal treed bog: Responses to warming and water-table-lowering simulations of climate change, *Biogeosciences*, 12, 1091–1111, <https://doi.org/10.5194/bg-12-1091-2015>, 2015.
- 1025 Neubauer, S. C. and Megonigal, J. P.: Moving Beyond Global Warming Potentials to Quantify the Climatic Role of Ecosystems, *Ecosystems*, 18, 1000–1013, <https://doi.org/10.1007/s10021-015-9879-4>, 2015.
- Nieveen, J. P., Campbell, D. I., Schipper, L. A., and Blair, I. J.: Carbon exchange of grazed pasture on a drained peat soil, *Global Change Biology*, 11, 607–618, <https://doi.org/10.1111/j.1365-2486.2005.00929.x>, 2005.
- 1030 Noumonvi, K. D., Ågren, A. M., Ratcliffe, J. L., Öquist, M. G., Ericson, L., Tong, C. H. M., Järveoja, J., Zhu, W., Osterwalder, S., Peng, H., Erefur, C., Bishop, K., Laudon, H., Nilsson, M. B., and Peichl, M.: The Kulbäcksliden Research Infrastructure: a unique setting for northern peatland studies, *Front. Earth Sci.*, 11, 1194749, <https://doi.org/10.3389/feart.2023.1194749>, 2023.
- 1035 Oehri, J., Schaepman-Strub, G., Kim, J.-S., Grysko, R., Kropp, H., Grünberg, I., Zemlianskii, V., Sonnentag, O., Euskirchen, E. S., Reji Chacko, M., Muscari, G., Blanken, P. D., Dean, J. F., di Sarra, A., Harding, R. J., Sobota, I., Kutzbach, L., Plekhanova, E., Riihelä, A., Boike, J., Miller,

- 1040 N. B., Beringer, J., López-Blanco, E., Stoy, P. C., Sullivan, R. C., Kejna, M., Parmentier, F.-J. W., Gamon, J. A., Mastepanov, M., Wille, C., Jackowicz-Korczynski, M., Karger, D. N., Quinton, W. L., Putkonen, J., van As, D., Christensen, T. R., Hakuba, M. Z., Stone, R. S., Metzger, S., Vandecrux, B., Frost, G. V., Wild, M., Hansen, B., Meloni, D., Domine, F., te Beest, M., Sachs, T., Kalhori, A., Rocha, A. V., Williamson, S. N., Morris, S., Atchley, A. L., Essery, R., Runkle, B. R. K., Holl, D., Riihimaki, L. D., Iwata, H., Schuur, E. A. G., Cox, C. J., Grachev, A. A., McFadden, J. P., Fausto, R. S., Göckede, M., Ueyama, M., Pirk, N., de Boer, G., Bret-Harte, M. S., Leppäranta, M., Steffen, K., Friborg, T., Ohmura, A., Edgar, C. W., 1045 Olofsson, J., and Chambers, S. D.: Vegetation type is an important predictor of the arctic summer land surface energy budget, *Nat Commun*, 13, 6379, <https://doi.org/10.1038/s41467-022-34049-3>, 2022.
- 1050 Ofiti, N. O. E., Schmidt, M. W. I., Abiven, S., Hanson, P. J., Iversen, C. M., Wilson, R. M., Kostka, J. E., Wiesenberg, G. L. B., and Malhotra, A.: Climate warming and elevated CO₂ alter peatland soil carbon sources and stability, *Nat Commun*, 14, 7533, <https://doi.org/10.1038/s41467-023-43410-z>, 2023.
- Page, S. E., Rieley, J. O., and Banks, C. J.: Global and regional importance of the tropical peatland carbon pool, *Global Change Biology*, 17, 798–818, <https://doi.org/10.1111/j.1365-2486.2010.02279.x>, 2011.
- 1055 Peacock, M., Audet, J., Bastviken, D., Futter, M. N., Gauci, V., Grinham, A., Harrison, J. A., Kent, M. S., Kosten, S., Lovelock, C. E., Veraart, A. J., and Evans, C. D.: Global importance of methane emissions from drainage ditches and canals, *Environ. Res. Lett.*, 16, 044010, <https://doi.org/10.1088/1748-9326/abeb36>, 2021.
- 1060 Peylin, P., Bacour, C., MacBean, N., Leonard, S., Rayner, P., Kuppel, S., Koffi, E., Kane, A., Maignan, F., Chevallier, F., Ciais, P., and Prunet, P.: A new stepwise carbon cycle data assimilation system using multiple data streams to constrain the simulated land surface carbon cycle, *Geosci. Model Dev.*, 9, 3321–3346, <https://doi.org/10.5194/gmd-9-3321-2016>, 2016.
- 1065 Prananto, J. A., Minasny, B., Comeau, L., Rudiyanto, R., and Grace, P.: Drainage increases CO₂ and N₂ O emissions from tropical peat soils, *Global Change Biology*, 26, 4583–4600, <https://doi.org/10.1111/gcb.15147>, 2020.

- 1070 Qiu, C., Zhu, D., Ciais, P., Guenet, B., Krinner, G., Peng, S., Aurela, M., Bernhofer, C., Brümmer, C., Bret-Harte, S., Chu, H., Chen, J., Desai, A. R., Dušek, J., Euskirchen, E. S., Fortuniak, K., Flanagan, L. B., Friborg, T., Grygoruk, M., Gogo, S., Grünwald, T., Hansen, B. U., Holl, D., Humphreys, E., Hurkuck, M., Kiely, G., Klatt, J., Kutzbach, L., Langeron, C., Laggoun-Défarge, F., Lund, M., Lafleur, P. M., Li, X., Mammarella, I., Merbold, L., Nilsson, M. B., Olejnik, J., Ottosson-Löfvenius, M., Oechel, W., Parmentier, F.-J. W., Peichl, M., Pirk, N., Peltola, O., Pawlak, W., Rasse, D., Rinne, J., Shaver, G., Schmid, H. P., Sottocornola, M., Steinbrecher, R., Sachs, T., Urbaniak, M., Zona, D., and Ziemblinska, K.: ORCHIDEE-PEAT (revision 4596), a model for northern peatland CO₂, water, and energy fluxes on daily to annual scales, *Geosci. Model Dev.*, 11, 497–519, <https://doi.org/10.5194/gmd-11-497-2018>, 2018.
- 1075 Qiu, C., Zhu, D., Ciais, P., Guenet, B., Peng, S., Krinner, G., Tootchi, A., Ducharne, A., and Hastie, A.: Modelling northern peatland area and carbon dynamics since the Holocene with the ORCHIDEE-PEAT land surface model (SVN r5488), *Geosci. Model Dev.*, 12, 2961–2982, <https://doi.org/10.5194/gmd-12-2961-2019>, 2019.
- 1080 Qiu, C., Ciais, P., Zhu, D., Guenet, B., Peng, S., Petrescu, A. M. R., Lauerwald, R., Makowski, D., Gallego-Sala, A. V., Charman, D. J., and Brewer, S. C.: Large historical carbon emissions from cultivated northern peatlands, *Sci. Adv.*, 7, eabf1332, <https://doi.org/10.1126/sciadv.abf1332>, 2021.
- 1085 Renou-Wilson, F., Müller, C., Moser, G., and Wilson, D.: To graze or not to graze? Four years greenhouse gas balances and vegetation composition from a drained and a rewetted organic soil under grassland, *Agriculture, Ecosystems & Environment*, 222, 156–170, <https://doi.org/10.1016/j.agee.2016.02.011>, 2016.
- 1090 Rojstaczer, S. and Deverel, S. J.: Time dependence in atmospheric carbon inputs from drainage of organic soils, *Geophysical Research Letters*, 20, 1383–1386, <https://doi.org/10.1029/93GL01339>, 1993.
- Rosset, T., Binet, S., Rigal, F., and Gandois, L.: Peatland Dissolved Organic Carbon Export to Surface Waters: Global Significance and Effects of Anthropogenic Disturbance, *Geophysical Research Letters*, 49, e2021GL096616, <https://doi.org/10.1029/2021GL096616>, 2022.

- 1095 Roulet, N. T. and Moore, T. R.: The effect of forestry drainage practices on the emission of methane from northern peatlands, *Can. J. For. Res.*, 25, 491–499, <https://doi.org/10.1139/x95-055>, 1995.
- Rydin, H. and Jeglum, J. K.: *The Biology of Peatlands*, Oxford University Press, <https://doi.org/10.1093/acprof:osobl/9780199602995.001.0001>, 2013.
- Salmon, E., Jégou, F., Guenet, B., Jourdain, L., Qiu, C., Bastrikov, V., Guimbaud, C., Zhu, D., Ciais, P., Peylin, P., Gogo, S., Laggoun-Défarge, F., Aurela, M., Bret-Harte, M. S., Chen, J., Chojnicki, B. H., Chu, H., Edgar, C. W., Euskirchen, E. S., Flanagan, L. B., Fortuniak, K., Holl, D., Klatt, J., Kolle, O., Kowalska, N., Kutzbach, L., Lohila, A., Merbold, L., Pawlak, W., Sachs, T., and Ziemblínska, K.: Assessing methane emissions for northern peatlands in ORCHIDEE-PEAT revision 7020, *Geosci. Model Dev.*, 15, 2813–2838, <https://doi.org/10.5194/gmd-15-2813-2022>, 2022.
- 1100 Saurich, A., Tiemeyer, B., Don, A., Fiedler, S., Bechtold, M., Amelung, W., and Freibauer, A.: Drained organic soils under agriculture — The more degraded the soil the higher the specific basal respiration, *Geoderma*, 355, 113911, <https://doi.org/10.1016/j.geoderma.2019.113911>, 2019.
- 1110 Schilstra, A. J. and Gerding, M. A. W.: Peat Resources, in: *Encyclopedia of Energy*, Elsevier, 805–810, <https://doi.org/10.1016/B0-12-176480-X/00567-2>, 2004.
- Sirin, A., Chistotin, M., Suvorov, G., Glagolev, M., Kravchenko, I., and Minaeva, T.: *Drained peatlands used for extraction and agriculture: biogeochemical status with special attention to greenhouse gas fluxes and rewetting*, 2010.
- 1115 Smola, A. J. and Schölkopf, B.: A tutorial on support vector regression, *Statistics and Computing*, 14, 199–222, <https://doi.org/10.1023/B:STCO.0000035301.49549.88>, 2004.
- Strack, M. and Waddington, J. M.: Response of peatland carbon dioxide and methane fluxes to a water table drawdown experiment, *Global Biogeochemical Cycles*, 21, 2006GB002715, <https://doi.org/10.1029/2006GB002715>, 2007.
- 1120 Swails, E. E., Ardón, M., Krauss, K. W., Peralta, A. L., Emanuel, R. E., Helton, A. M., Morse, J. L., Gutenberg, L., Cormier, N., Shoch, D., Settlemyer, S., Soderholm, E., Boutin, B. P., Peoples, C., and Ward, S.: Response of soil respiration to changes in soil temperature and water table

level in drained and restored peatlands of the southeastern United States, *Carbon Balance Manage*, 17, 18, <https://doi.org/10.1186/s13021-022-00219-5>, 2022.

- 1125 Tarantola, A.: *Inverse Problem Theory and Methods for Model Parameter Estimation*, SIAM, 349 pp., 2005.
- Tikkasalo, O.-P., Peltola, O., Alekseychik, P., Heikkinen, J., Launiainen, S., Lehtonen, A., Li, Q., Martinez-García, E., Peltoniemi, M., Salovaara, P., Tuominen, V., and Mäkipää, R.: Eddy covariance fluxes of CO₂, CH₄ and N₂O on a drained peatland forest after clearcutting, <https://doi.org/10.5194/egusphere-2024-1994>, 15 August 2024.
- 1130 Tong, C. H. M., Noumonvi, K. D., Ratcliffe, J., Laudon, H., Järveoja, J., Drott, A., Nilsson, M. B., and Peichl, M.: A drained nutrient-poor peatland forest in boreal Sweden constitutes a net carbon sink after integrating terrestrial and aquatic fluxes, *Global Change Biology*, 30, e17246, <https://doi.org/10.1111/gcb.17246>, 2024.
- 1135 Truskavetskii, R. S.: Carbon budget of drained peat bogs in Ukrainian Polesie, *Eurasian Soil Sc.*, 47, 687–693, <https://doi.org/10.1134/S1064229314050238>, 2014.
- Ueyama, M., Hirano, T., and Kominami, Y.: FLUXNET-CH₄ JP-BBY Bibai bog, <https://doi.org/10.18140/FLX/1669646>, 2020.
- Villa, J. A., Mejía, G. M., Velásquez, D., Botero, A., Acosta, S. A., Marulanda, J. M., Osorno, A. M., and Bohrer, G.: Carbon sequestration and methane emissions along a microtopographic gradient in a tropical Andean peatland, *Science of The Total Environment*, 654, 651–661, <https://doi.org/10.1016/j.scitotenv.2018.11.109>, 2019.
- 1140 Waddington, J. M., Morris, P. J., Kettridge, N., Granath, G., Thompson, D. K., and Moore, P. A.: Hydrological feedbacks in northern peatlands, *Ecohydrology*, 8, 113–127, <https://doi.org/10.1002/eco.1493>, 2015.
- 1145 Xi, Y., Qiu, C., Zhang, Y., Zhu, D., Peng, S., Hugelius, G., Chang, J., Salmon, E., and Ciais, P.: Assessment of a tiling energy budget approach in a land surface model, ORCHIDEE-MICT (r8205), *Geoscientific Model Development*, 17, 4727–4754, <https://doi.org/10.5194/gmd-17-4727-2024>, 2024.
- 1150 Zou, J., Ziegler, A. D., Chen, D., McNicol, G., Ciais, P., Jiang, X., Zheng, C., Wu, J., Wu, J., Lin, Z., He, X., Brown, L. E., Holden, J., Zhang, Z., Ramchunder, S. J., Chen, A., and Zeng, Z.:

Rewetting global wetlands effectively reduces major greenhouse gas emissions, *Nat. Geosci.*, 15, 627–632, <https://doi.org/10.1038/s41561-022-00989-0>, 2022.

Appendix A

155

Table A1: The 12 peatland sites used in this study for virtual drainage simulations. Their locations were mapped in Fig. A1. A star (*) beside a site ID indicates flux and WTD observations sourced from the FLUXNET-CH4 database; otherwise, these observations are from the Wet Horizons project. The vegetation composition (graminoids, shrubs, and mosses) is taken from the literature when available; otherwise, it is estimated visually from satellite images.

Site ID	Lat, lon	Type	Peat-graminoids/shrub/moss fraction	CO ₂ flux observation	CH ₄ flux observation	WTD observation	References
CA-SCB*	61.31, -121.30	Bog, pristine	0.2 / 0.2 / 0.6	2014-2017		Yes	(Oehri et al., 2022)
CZ-Wet	49.02, 14.77	Fen, pristine	0.8 / 0.2 / 0	2021-2022	None	No	(Mejdová et al., 2021)
DE-Akm	53.87, 13.68	Fen, near-natural	0.5 / 0.5 / 0	2009-2014	None	No	(Bernhofer et al., 2009)
FI-Sii	61.83, 24.19	Fen, pristine	0.26 / 0.1 / 0.64	2018-2021		Yes	(Aurela et al., 2007)
JP-BBY*	43.32, 141.81	Bog, pristine	0.2 / 0.2 / 0.6	2015-2018		Yes	(Ueyama et al., 2020)
SE-Deg	64.18, 19.56	Fen, pristine	0.44 / 0.11 / 0.45	2020-2022		Yes	(Noumonvi et al., 2023)
SE-HfM	64.16, 19.55	Fen, pristine	0.5 / 0.07 / 0.43	2020-2022		Yes	(Noumonvi et al., 2023)
SE-Hmr	64.16, 19.57	Fen, pristine	0.36 / 0.21 / 0.43	2020-2022		Yes	(Noumonvi et al., 2023)

SE-Srj	64.17, 19.56	Fen, pristine	0.37 / 0.15 / 0.48	2020-2022	Yes	(Noumonvi et al., 2023)
US-Los*	46.08, -89.98	Fen, pristine	0.5 / 0.1 / 0.4	2014-2018	Yes	(Desai and Thom, 2020)

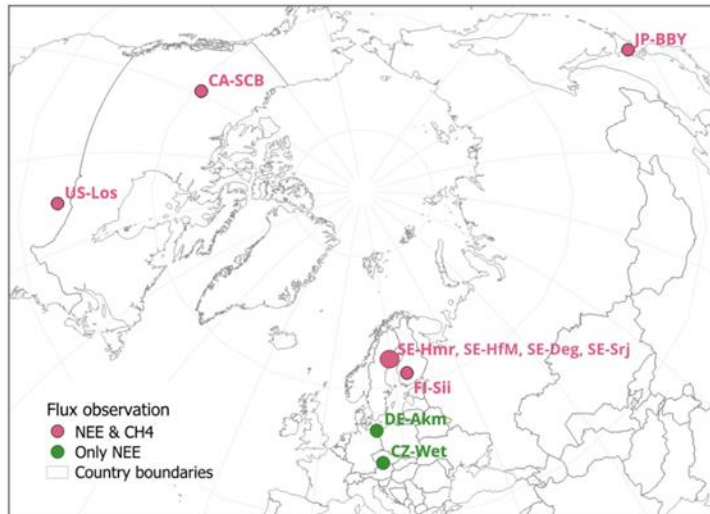


Figure A1. Location of peatland sites. Figure contains public sector information licensed under the Open Government Licence v3.0.

Appendix B

Table B1. Parameters for model calibration. The PFT column uses G, S, and M to denote graminoids, shrubs, and mosses, respectively, and "-" for parameters that are independent of PFTs. For further details, refer to Liu et al. (2025) for parameters related to photosynthesis, autotrophic respiration, and SOC decomposition, and to (Salmon et al., 2022) for methane-related processes.

Parameter	Description	PFT
Photosynthesis		
VC_{max}	Maximum rate of carboxylation	G, S, M
LAI_{max}	Maximum leaf area index	G, S, M
SLA	Specific leaf area	G, S, M
g_0	Stomatal conductance of mosses when no irradiance	M
a_1	Empirical constants	M
b_1	Empirical constants	M
	Autotrophic respiration	
$C_{0,leaf}$	Maintenance respiration coefficient at 0 °C for leaves	G, S, M
GR_{frac}	Fraction of biomass allocated to growth respiration	G, S, M
SOC decomposition		
T_{peat}	Carbon decomposition rate parameter for peat vegetation	G, S, M
Q_{10}	Temperature sensitivity coefficient of the decomposition rate	-
Methane-related processes		
q_{MG}	Ratio of soil oxic and anoxic decomposition	-
k_{MT}	Methanotrophy rate	-
M_{rox}	Root methane oxidation	G, S, M

Parameter	Description	PFT
Z_{root}	Root depth	G, S, M
T_{veg}	The efficiency of methane plant mediated transport	G, S, M
wsize	Connectivity of soil moisture	-
m_{XRCH_4}	Methane mixing ratio in bubbles	-
O2m	Oxygen concentration below which anoxic condition is reached for methane production	-

1170

Appendix C

Text C1. Akaike information criterion (AIC).

1175 The AIC (Akaike, 1974) is a statistical metric used to evaluate the relative quality of different
models for a given dataset by estimating the trade-off between the goodness of fit and model
complexity, with lower AIC values indicating a better trade-off. For each model, AIC is calculated
by:

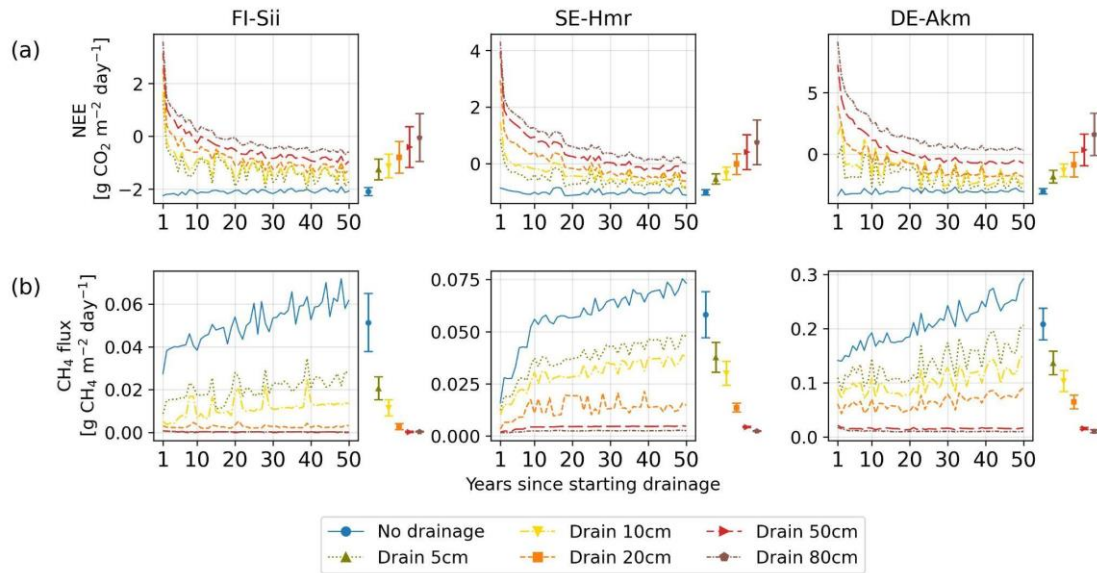
$$AIC = 2K - 2\ln(L) \quad (C1)$$

1180 where K is the number of estimated parameters in the model and L is the maximum value of the
likelihood function for the model, reflecting how well the model fits the data.

The corrected Akaike information criterion (AICc) adjusts the standard AIC to account for small
sample sizes (e.g. 10 samples in Sect. 3.7 of this study), ensuring better reliability of model
comparisons when the sample size (n) is relatively low compared to the number of model parameters
(K). The formula for AICc is:

1185

$$AICc = AIC + \frac{2K(K+1)}{n-K-1} \quad (C2)$$



1190 **Figure C1.** Simulated time series of (a) net ecosystem exchange (NEE) of CO₂ and (b) CH₄ emissions over the 50-year simulation period at the same three sites as in Fig. 4. Different colors and line styles indicate different water table depths below the original water level at each site. The colored bar shown to the right of each panel summarizes uncertainty arising from parameter uncertainty, expressed as ± 1 standard deviation of the simulated time-mean flux over the 50-year simulation period. The colored dots indicate the corresponding time-mean flux simulated using the calibrated parameter set. Note that when a flux (e.g. CH₄) is close to zero, the corresponding parameter-induced uncertainty also approaches zero.

1195

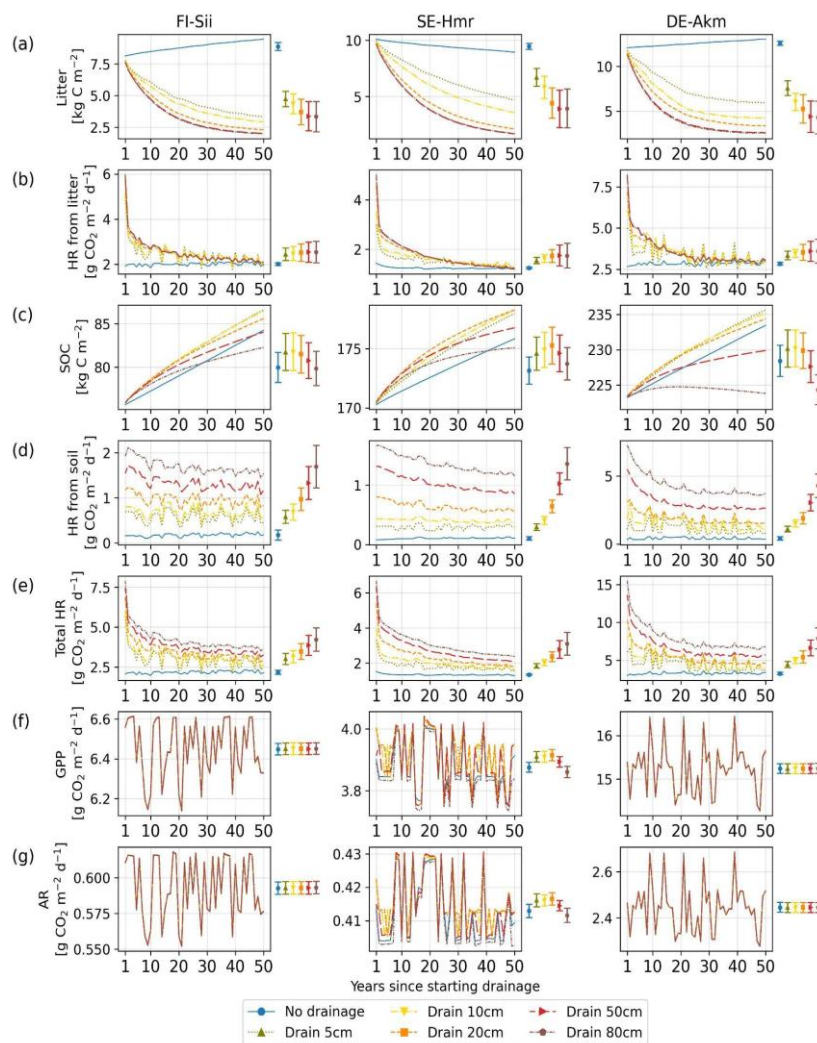
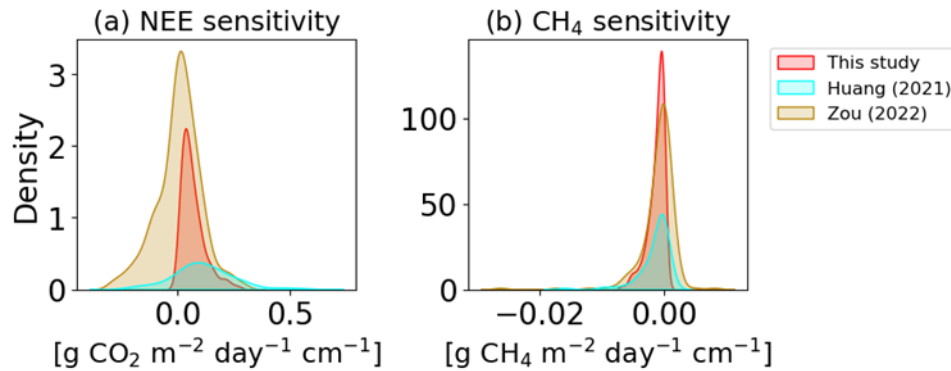
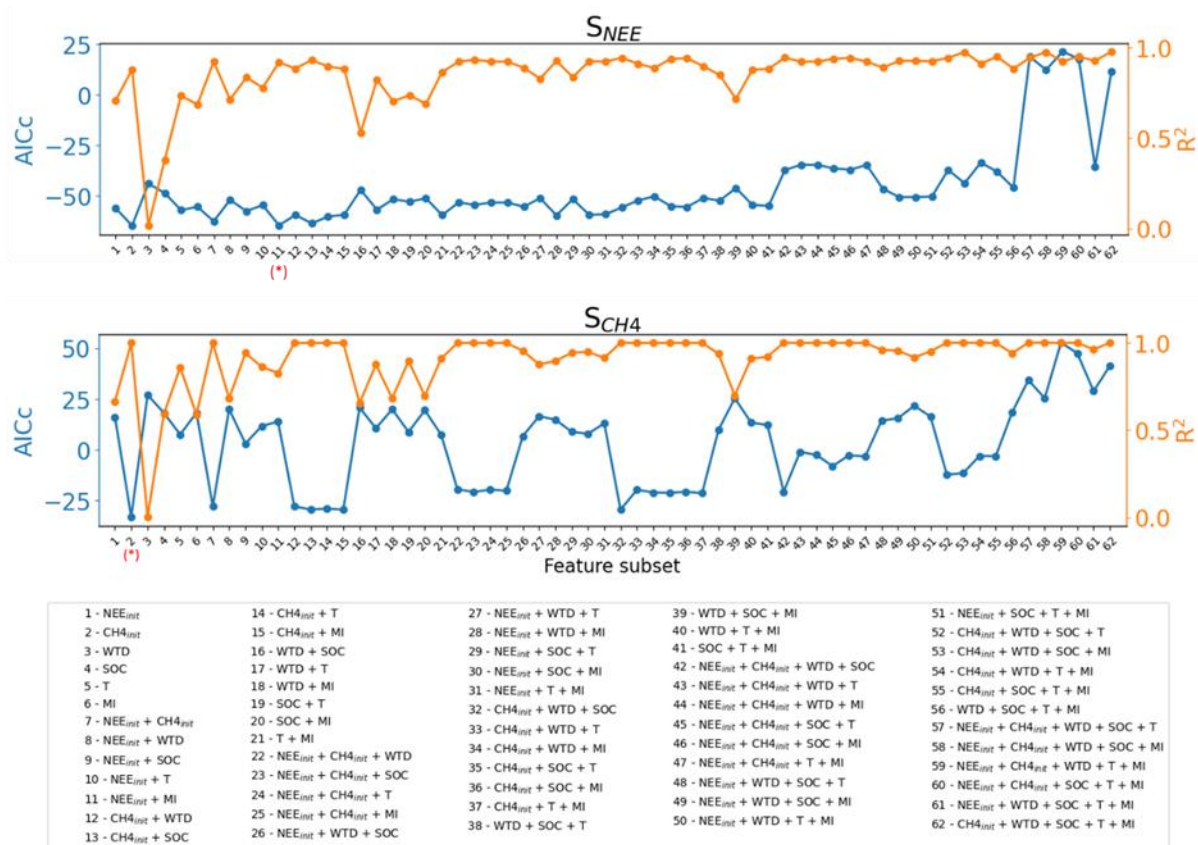


Figure C2. Simulated changes in litter carbon and soil organic carbon (SOC) pools and associated heterotrophic respiration over the 50-year simulation period following the onset of drainage. Shown are (a) litter carbon, (b) heterotrophic respiration (HR) from litter, (c) soil organic carbon, (d) heterotrophic respiration from soil, (e) total heterotrophic respiration (sum of litter and soil components), (f) gross primary production (GPP), and (g) autotrophic respiration (AR) at three sites. Different colors and line styles indicate different water table depths below the original water level at each site. The coloured bars on the right of each panel summarize parameter uncertainty, quantified as ± 1 standard deviation of the simulated time-mean fluxes computed over the full 50-year simulation from 10 Monte Carlo runs. The colored dots indicate the corresponding time-mean flux simulated using the calibrated parameter set. Note that when a flux (e.g. HR) is close to zero, the corresponding parameter-induced uncertainty also approaches zero.



1210 **Figure C3:** Distribution of sensitivities of (a) net ecosystem exchange (NEE) and (b) CH₄ emissions
 1215 to water table drawdown across peatland sites. Results from this study are compared with reference
 datasets from Huang et al. (2021) and Zou (2022). Sensitivities are expressed as changes in flux per
 centimeter of water table drawdown ($\Delta\text{flux}/\Delta\text{WTD}$). Modeled results are based on drainage
 simulations over the first 10 years, consistent with the temporal window used for sensitivity analysis
 in **Fig. 7–9**.



1220 **Figure C4.** Selection of explanatory variable subsets for the sensitivities of net ecosystem exchange (S_{NEE}) and CH_4 emissions (S_{CH_4}). For each possible subset of predictor variables, the corrected Akaike Information Criterion (AICc; blue lines, left axis) and the coefficient of determination (R^2 ; orange lines, right axis) are shown. Lower AICc values indicate better model parsimony. The red star marks the variable subset selected for the exploratory emulator presented in Eqs. (3) and (4).

1225

Table C1: Coefficient of determination (R^2) and p-values from leave-one-out fitting of Eq.3 and Eq.4, with the site removed indicated in the first column.

Site removed	Fitting Eq (3)		Fitting Eq (4)	
	R^2	p-value	R^2	p-value
CA-SCB	0.913	0.0007	0.997	10^{-6}
CZ-Wet	0.914	0.0006	0.998	10^{-8}
DE-Akm	0.858	0.0028	0.998	10^{-8}
FI-Sii	0.925	0.0004	0.999	10^{-7}
JP-BBY	0.947	0.0002	0.994	10^{-6}
SE-Deg	0.933	0.0003	0.999	10^{-7}
SE-HfM	0.922	0.0005	0.998	10^{-7}
SE-Hmr	0.917	0.0006	0.998	10^{-7}
SE-Srj	0.912	0.0007	0.998	10^{-7}
US-Los	0.937	0.0003	0.998	10^{-7}
Mean \pm STD	0.918 ± 0.023	0.0007 ± 0.0007	0.998 ± 0.001	$10^{-7} \pm 10^{-7}$

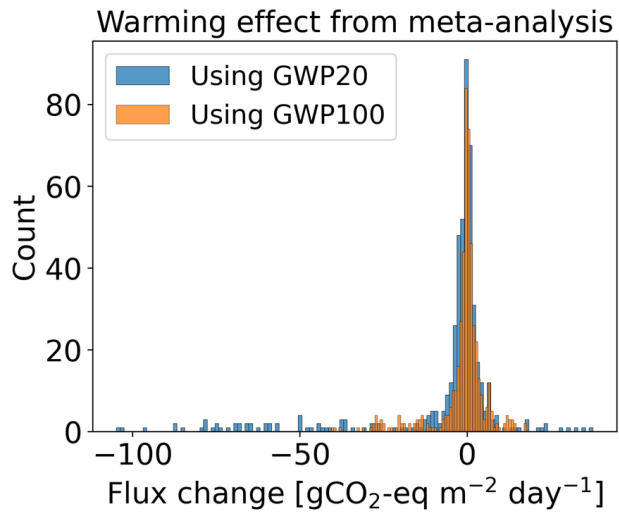


Figure C5. Distribution of flux change in CO₂-eq from meta-analysis data.

1230

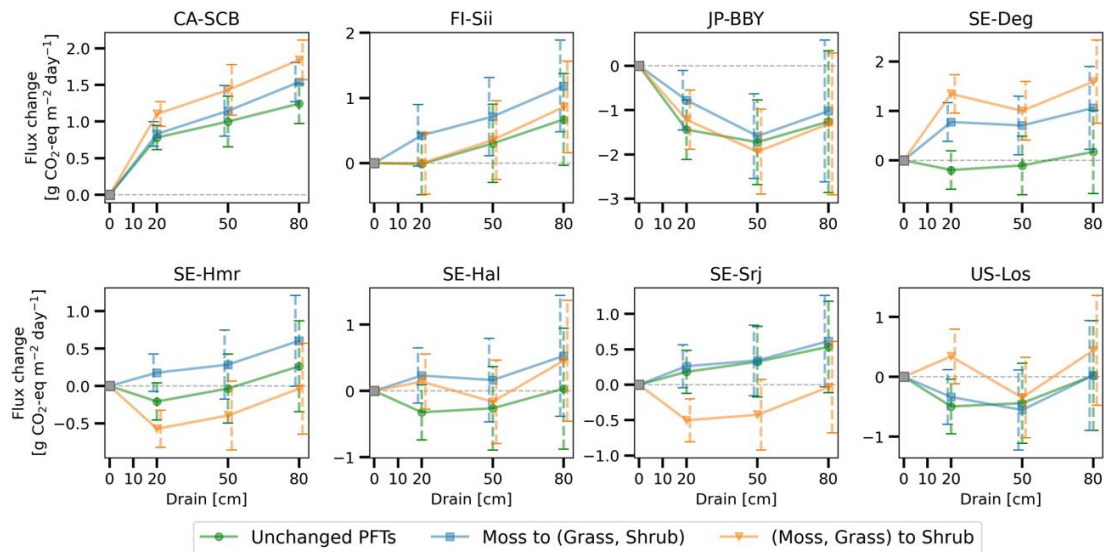
Appendix D

Site-level current vegetation composition was first adjusted to match available field observations, providing a realistic baseline for model initialization. However, the trajectory of vegetation change following peatland drainage remains highly uncertain, and no single future vegetation scenario can be considered more likely than others. To account for this uncertainty, we evaluated two alternative vegetation change scenarios in addition to the baseline scenario with unchanged plant functional types (PFTs). Results from these three vegetation scenarios were combined to form an ensemble, with the mean response reported in the main analysis and the minimum–maximum range used to quantify vegetation-related uncertainty. Two peatland vegetation change scenarios were applied to all sites, except CZ-Wet and DE-Akm, where mosses are absent from the PFT composition:

(1) After 10 years of drainage, 50% of moss was replaced by grass and shrub; after 20 years, all moss was fully replaced by grass and shrub.

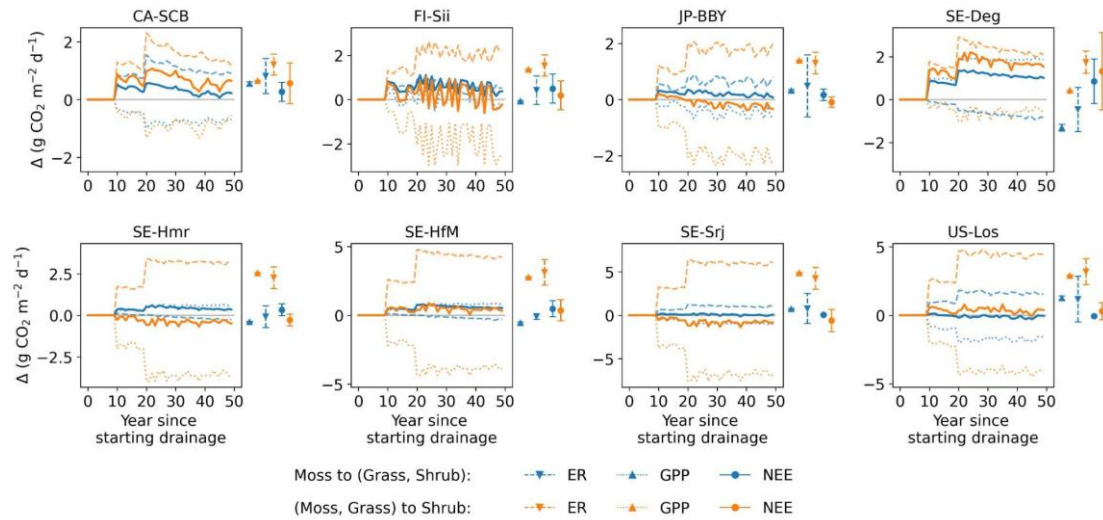
(2) After 10 years of drainage, 50% of moss and grass was replaced by shrub; after 20 years, both moss and grass were entirely replaced by shrub.

The combined effects over 50 years using GWP100 (similar to **Fig. 10**) are shown in **Fig. D1**. At site CA-SCB, FI-Sii, and JP-BBY, both vegetation shifts had slight impacts - drainage still resulted in warming effect at CA-SCB and FI-Sii, and cooling effects at JP-BBY. The conversion of moss to other peatland PFTs had little impact at SE-Srj and US-Los, but led to significantly increased drainage-induced CO₂-equivalent emission in SE-Deg, SE-Hmr, and SE-HfM (moving up from green to blue lines). The conversion of moss and grass to shrub caused more variations at these five sites (orange lines): drainage can cause a cooling effect instead of warming (e.g. at SE-Hmr, SE-Srj) or vice versa (e.g. at SE-Deg, SE-HfM). These results highlight the importance of accounting for vegetation dynamics in future modelling. Changes in CO₂ and CH₄ fluxes under the vegetation change scenarios (relative to the unchanged PFT scenario) are illustrated in **Fig. D2** and **D3** for the 80 cm drainage case, with the CO₂-equivalent emission of the three vegetation scenarios shown in **Fig. D4**.

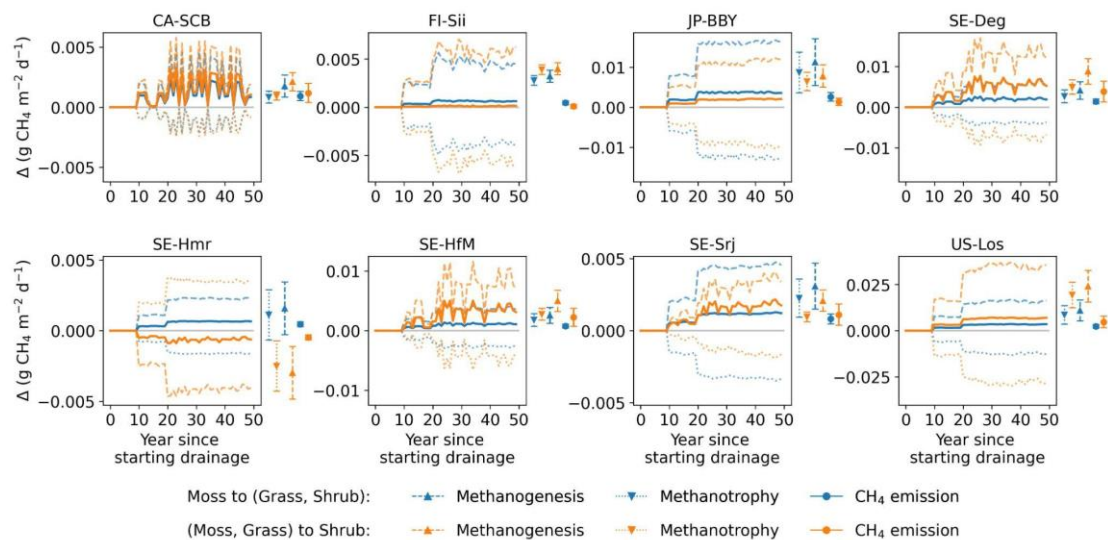


1260 **Figure D1.** Combined effect of drainage over a 50-year period evaluated using GWP100 under three vegetation scenarios: unchanged plant functional types (PFTs; green), conversion of moss to grass and shrubs (blue), and conversion of moss and grass to shrubs (orange). Error bars show parameter uncertainty (± 1 standard deviation of 50-year time-mean CO_2 -equivalent fluxes across 10 Monte Carlo runs). Because all vegetation scenarios use the same baseline-calibrated parameter set and model structure, parameter uncertainty is identical across scenarios, whereas differences among curves reflect vegetation scenario uncertainty.

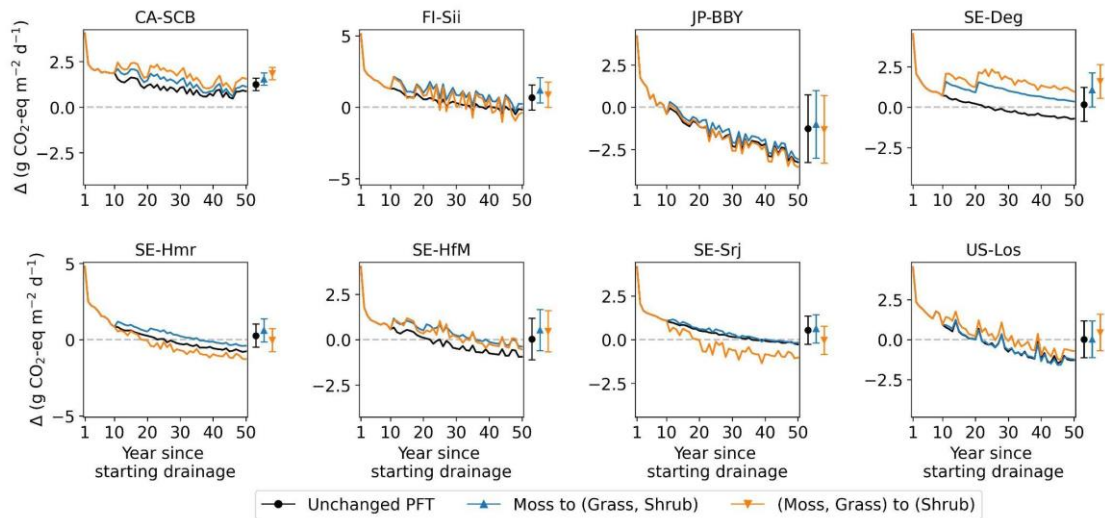
1265



1270 **Figure D2.** Changes in gross primary production (GPP), ecosystem respiration (ER), and net
ecosystem exchange (NEE) under two vegetation change scenarios, relative to the unchanged plant
functional type (PFT) scenario, for the 80 cm drainage case. Results are shown for the conversion
of moss to grass and shrubs and for the conversion of moss and grass to shrubs. All vegetation
scenarios were simulated using the same baseline-calibrated parameter set and model structure; ;
therefore, parameter uncertainty is identical across vegetation scenarios. The coloured bars shown
to the right of each panel represent parameter uncertainty, quantified as ± 1 standard deviation of the
1275 simulated time-mean fluxes over the full 50-year simulation period across 10 Monte Carlo runs. The
colored dots indicate the corresponding time-mean flux simulated using the calibrated parameter
set.



1280 **Figure D3.** Changes in methanogenesis, methane oxidation (methanotrophy), and net CH₄
 1285 emissions under two vegetation change scenarios, relative to the unchanged plant functional type
 (PFT) scenario, for the 80 cm drainage case. Results are shown for the conversion of moss to grass
 and shrubs and for the conversion of moss and grass to shrubs. All vegetation scenarios were
 simulated using the same baseline-calibrated parameter set and model structure; therefore,
 parameter uncertainty is identical across vegetation scenarios. The coloured bars shown to the right
 of each panel represent parameter uncertainty, quantified as ± 1 standard deviation of the simulated
 time-mean fluxes over the full 50-year simulation period across 10 Monte Carlo runs. The colored
 dots indicate the corresponding time-mean flux simulated using the calibrated parameter set.



1290

1295

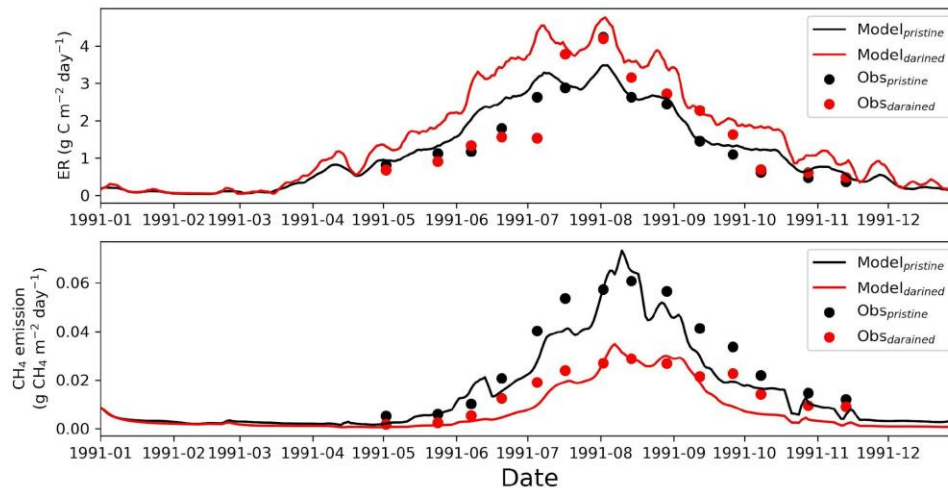
Figure D4. CO₂-equivalent emissions under two vegetation change scenarios for the 80 cm drainage case: unchanged plant functional types (PFTs), conversion of moss to grass and shrubs, and conversion of moss and grass to shrubs. All vegetation scenarios were simulated using the same baseline-calibrated parameter set and model structure; therefore, parameter uncertainty is identical across vegetation scenarios. The coloured bars shown to the right of each panel represent parameter uncertainty, quantified as ± 1 standard deviation of the simulated time-mean CO₂-equivalent fluxes over the full 50-year simulation period across 10 Monte Carlo runs. The colored dots indicate the corresponding time-mean flux simulated using the calibrated parameter set.

1300 **Appendix E**

To demonstrate the reliability of the drainage model, we evaluated its performance against available field observations. Although paired drainage experiments with comprehensive and long-term flux measurements are rare, we compiled warm-season (1991) field observations of both ecosystem respiration (ER) and CH₄ emissions from a site located near FI-Sii and
1305 conducted a dedicated simulation experiment. This site has experienced peatland drainage for approximately 40 years prior to the observation period (Nykänen et al., 1998; Kwon et al., 2022). During the 1991 measurement period, the drained treatment exhibited a water table depth (WTD) approximately 10 cm lower than that of the pristine (control) condition.

Model parameters were first calibrated using observed fluxes from the pristine condition,
1310 following the calibration protocol described in the main text. The calibrated model was then applied to simulate the drainage scenario by prescribing a WTD that was approximately 10 cm lower than the pristine condition, consistent with the observed WTD difference during the 1991 campaign. A comparison between modeled and observed ER and CH₄ emissions is shown in Fig. E1. The model reproduces the observed changes in fluxes between pristine and drained
1315 conditions reasonably well, particularly for CH₄ emissions.

Overall, this experiment provides independent support that the model is capable of capturing drainage-induced changes in greenhouse gas fluxes under real-world conditions.



1320 **Figure E1.** Comparison of observed and modeled ecosystem respiration (ER) and CH₄ emissions of a drainage experiment near the pristine peat site of FI-Sii. The drained conditions are in red, and the controls (pristine peat) are in black. Lines are our simulations, and dots are the observed fluxes.